Evolving Systems (2022) 13:243–264
https://doi.org/10.1007/s12530-021-09381-6

ORIGINAL PAPER

A novel interval type-2 fuzzy Kalman filtering and tracking of experimental data

Daiana Caroline dos Santos Gomes[1] · **Ginalber Luiz de Oliveira Serra**[2]

Received: 29 July 2020 / Accepted: 9 April 2021 / Published online: 28 April 2021

Abstract
In this paper, a methodology for design of fuzzy Kalman filter, using interval type-2 fuzzy models, in discrete time domain, via spectral decomposition of experimental data, is proposed. The adopted methodology consists of recursive parametric estimation of local state space linear submodels of interval type-2 fuzzy Kalman filter for tracking and forecasting of the dynamics inherited to experimental data, using an interval type-2 fuzzy version of Observer/Kalman Filter Identification (OKID) algorithm. The partitioning of the experimental data is performed by interval type-2 fuzzy Gustafson–Kessel clustering algorithm. The interval Kalman gains in the consequent proposition of interval type-2 fuzzy Kalman filter are updated according to unobservable components computed by recursive spectral decomposition of experimental data. Computational results illustrate the efficiency of proposed methodology for filtering and tracking the time delayed state variables of Chen's chaotic attractor in a noisy environment, and experimental results illustrate its applicability for adaptive and real time forecasting the dynamic spread behavior of novel Coronavirus 2019 (COVID-19) outbreak in Brazil.

Keywords Systems identification · Interval type-2 fuzzy systems · Recursive parametric estimation · Kalman filtering

1 Introduction

In sciences and engineering is very common the solution of problems with stochastic nature such as prediction, separation and detection of signals in the presence of random noise (Mack and Habets 2020; Gomez-Garcia et al. 2020; Liu et al. 2019; Zhu et al. 2019; Chen et al. 2005; Hsieh 2000). Kalman filter (KF) is the most well known and used mathematical tool for stochastic estimation from noisy and uncertain measurements. It was proposed by Rudolph E. Kalman in 1960, who published his famous paper "A New Approach to Linear Filtering and Prediction Problem" (Kalman 1960), describing a recursive solution to discrete time linear filtering problem, and becoming a standard approach for optimal estimation. Since the time of its introduction, the Kalman filter has been the subject of extensive research and applications in the fields of orbit calculation, target tracking, integrated navigation, dynamic positioning, sensor data fusion, microeconomics, control, modeling, digital image processing, pattern recognition, image segmentation and image edge detection, and others. This broad interest in KF is due to its optimality, convenient form for online real-time processing, easy formulation and implementation (Serra 2018; Schimmack et al. 2018; Huang et al. 2018). The increasing in the complexity of practical dynamic systems has motivated researches in the sense of extending Kalman's filtering theory to face with nonlinearities and uncertainties, by using fuzzy systems theory, mainly the type-2 fuzzy systems, for applications in the area of modeling and control (Gil et al. 2019; Bouhentala et al. 2019; Hwang et al. 2019; Evangelista and Serra 2020; Serra 2018). These recent successful applications of type-2 fuzzy system are due to its structure based on rules, its capability of approximate functions, where the antecedent propositions describe fuzzy operation regions (uncertainties) and the consequent propositions express a nonlinear mapping of the physical behavior inherited to corresponding fuzzy operation regions (Zhang et al. 2020; Mendel 2019; Liang and Mendel 2000).

✉ Ginalber Luiz de Oliveira Serra
ginalber@ifma.edu.com

Daiana Caroline dos Santos Gomes
daianagomes159@gmail.com

[1] Federal University of Maranhão, Av. dos Portugueses, 1966, Vila Bacanga, São Luís, Maranhão CEP: 65080-805, Brazil

[2] Electrical Electronics Department, Federal Institute of Education, Science and Technology of Maranhão, Av. Getúlio Vargas, 04, Monte Castelo, São Luís, Maranhão CEP: 65030-005, Brazil

The proposed methodology in this paper is based on designing of Kalman filters using interval type-2 fuzzy models in the discrete time domain. A new formulation of type-2 fuzzy version of Observer/Kalman Filter Identification (OKID) algorithm, is proposed, for updating, recursively, the consequent proposition of type-2 fuzzy Kalman filter using spectral components extracted from the experimental data. Interval fuzzy sets characterizing the antecedent of type-2 fuzzy Kalman filter inference system are estimated by, also proposed, a formulation of interval type-2 fuzzy version of Gustafson-Kessel clustering algorithm. Computational results of filtering and tracking of a reference trajectory through state variables of a nonlinear dynamic system with chaotic behavior and time delays in a noisy environment shows the efficiency of proposed methodology as compared to other approach widely cited in the literature. The applicability of proposed methodology is illustrated through experimental results from real time interval tracking and forecasting of the COVID-19's dynamic spreading behavior in Brazil.

2 Related works

In the last years, studies involving the integration of fuzzy systems and Kalman filters have been proposed in the literature Pires and Serra (2019), Eyoh et al. (2018). In Wang et al. (2020), fuzzy sets are combined with an optimization method based on extended Kalman filter with probabilistic-numerical linguistic information applied for tracking a maneuvering target. According to limited and uncertain information from different sensors, the methodology is able to merge this information and be applied to the problem of trace optimization in an unknown maneuvering target in Sichuan province in China. In Asl et al. (2020), an optimization methodology of adaptive Unscented Kalman Filter (UKF) is presented by an evolutionary fuzzy algorithm named Fuzzy Adaptive Grasshopper Optimization Algorithm, and it is efficiently applied to different benchmark functions, such as robotic manipulator and servo-hydraulic system, whose performance is better compared to previous versions of UKF. Despite the extensive literature in these contexts, there are still many fields to be explored regarding the association of Kalman filters and fuzzy systems.

Applications involving the association of Kalman filters and type-2 fuzzy systems have also been developed in several areas in order for characterizing and reducing the effects of the uncertainties into dynamic systems (Evangelista and Serra 2019; Khanesar et al. 2012). In Lin et al. (2015), an interval type-2 neural fuzzy system is proposed, in which the consequent proposition weights are tuned via rule-ordered Kalman filter algorithm for enhancing learning effectiveness, using a self-evolving property that can automatically generate fuzzy rules and discard derogatory features when applied to the problem of systems identification. In Taghavifar (2020), an active suspension system for electric cars, based on type-2 fuzzy proportional-integral-derivative (PID) controller and extended Kalman filter is proposed for improving the vehicle design to accomplish an enhanced ride comfort and handle performance.

Differently from aforementioned approaches and others ones found from literature, the scope of this paper outlines the integration of Kalman filter and interval type-2 fuzzy systems for tracking and forecasting of uncertain experimental data. The design of interval type-2 fuzzy Kalman filter, according to proposed methodology, is based on spectral unobservable components and uncertainty regions extracted from experimental data of dynamic systems.

2.1 Motivation and contributions

Among the main aspects characterizing the complexity of problems in science and engineering are the nonlinearities (Bendat 1998; Schoukens and Ljung 2019), uncertainties (Martynyuk et al. 2019), noisy and non-stationary environment (Hendricks et al. 2008; Moss and McClintock 1989), temporal variability (Tomás-Rodríguez and Banks 2010), among others. Computational modeling approaches which consider these complexities in their formulations do have better performance for facing to conditions of stability and convergence (Bonyadi and Michalewicz 2016; Boutayeb et al. 1997), polarized parametric estimation (Chan et al. 2020; Haessig and Friedland 1998), non-modeled dynamics (Khayyam et al. 2020), high approximation and prediction errors (Tang et al. 2020). In data analysis, an increasingly concern from researchers is related to the presence of several types of uncertainties such as inaccuracy and incompleteness of data and information, parametric and structural uncertainties, propagation and accumulation of uncertainties, and unknown initial conditions, that must be taken into account by modeling approaches in order to ensure accurate models for real-world problems (Wang and Zhao 2013). Although recent studies have addressed the processing of uncertainties in the formulation of data analysis methodologies in different application domains such as engineering (Ma and Ma 2020), health (Heintzman and Kleinberg 2016), epidemiology (Gilbert et al. 2014), economics (Khairalla et al. 2018), among others, the research in this issue is still open. This has motivated the development of tools using fuzzy systems theory for data analysis (Hurtik et al. 2020; Lan et al. 2020; Pires and Serra 2020), mainly from the association of Kalman filters and type-2 fuzzy systems, which is the particular motivation of this paper in the sense of overcoming limitations of classic Kalman filtering to face high order nonlinearities, processing different types of uncertainties using interval fuzzy operation regions in non-stationary

experimental dataset, and guaranteeing a set of possible solutions within a confidence region.

The originality of proposed methodology is outlined by the following main contributions:

(a) A computational approach based on the successful integration of Kalman filters and type-2 fuzzy systems for adaptive tracking and real time forecasting of uncertain experimental dataset.
(b) Formulation of interval type-2 fuzzy clustering algorithm based on adaptive similarity distance mechanism able to define specific operation regions associated to the behavior and uncertainty inherent to experimental dataset.
(c) Formulation of computational model with intelligent machine learning based on interval type-2 fuzzy Kalman filter, for adaptive tracking and real time forecasting the behavior and uncertainty inherent to experimental dataset, from the specific operation regions defined in item "b".

3 Interval type-2 fuzzy computational model

In this section, the proposed methodology for designing the interval type-2 fuzzy Kalman filter computational model from experimental data, is presented. Formulations for pre-processing the experimental data by spectral analysis, parametric estimation of interval type-2 fuzzy Kalman filter antecedent proposition, parametric estimation of interval type-2 fuzzy Kalman filter consequent proposition and its recursive updating mechanism, are addressed.

3.1 Pre-processing by singular spectral analysis

The singular spectral analysis technique is a mathematical tool for analyzing and decomposing complex time series into simpler components within the original data. Such unobservable components have relevant characteristics about the corresponding time series behavior (Elsner 2002).

3.1.1 Training step

Let the initial experimental data set referring to p outputs of the dynamic system under analysis, with N_b samples, given by:

$$\mathbf{y} = [\mathbf{y}_1 \quad \mathbf{y}_2 \quad \cdots \quad \mathbf{y}_{N_b}], \quad \mathbf{y} \in \mathbb{R}^{p \times N_b} \tag{1}$$

where $\mathbf{y}_k \in \mathbb{R}^p$, with $k = 1, \ldots, N_b$, is the output vector of the dynamic system at instant of time k. From this initial data set, a trajectory matrix $\mathbf{H}$ is defined, for each of the dimensions of $\mathbf{y}$, considering a set of ρ delayed vectors with dimension δ, which is an integer number defined by user with $2 \leq \delta \leq N_b - 1$ and $\rho = N_b - \delta + 1$, given by:

$$\mathbf{H} = \begin{bmatrix} y_1 & y_2 & y_3 & \cdots & y_\rho \\ y_2 & y_3 & y_4 & \cdots & y_{\rho+1} \\ \vdots & \vdots & \vdots & \ddots & \vdots \\ y_\delta & y_{\delta+1} & y_{\delta+2} & \cdots & y_{N_b} \end{bmatrix}, \quad \mathbf{H} \in \mathbb{R}^{\delta \times \rho} \tag{2}$$

and the covariance matrix $\mathbf{S}$ is obtained as follows:

$$\mathbf{S} = \mathbf{H}\mathbf{H}^T, \qquad \mathbf{S} \in \mathbb{R}^{\delta \times \delta} \tag{3}$$

By applying the Singular Value Decomposition (SVD) procedure to covariance matrix $\mathbf{S}$, it is obtained as resulting variables a set of eigenvalues $\sigma^1 \geq \sigma^2 \geq \cdots \geq \sigma^\delta \geq 0$ and their respective eigenvectors, $\boldsymbol{\phi}^1, \boldsymbol{\phi}^2, \ldots, \boldsymbol{\phi}^\delta$, which represent the level of correlation between the experimental dataset and each spectral component to be extracted (Elsner 2002; Serra 2018).

Considering $d = max\{\varsigma, \text{such that } \sigma^\varsigma > 0\}$, and $\mathbf{V}^\varsigma = \mathbf{H}^T\boldsymbol{\phi}^\varsigma / \sqrt{\sigma^\varsigma}$ with $\varsigma = 1, \ldots, d$, the singular value decomposition of the trajectory matrix $\mathbf{H}$, can be rewritten as

$$\mathbf{H} = \mathbf{H}^1 + \mathbf{H}^2 + \cdots + \mathbf{H}^d \tag{4}$$

where the matrix $\mathbf{H}^\varsigma|^{\varsigma=1,\ldots,d}$ is elementary (it has rank equal to 1), and is given by:

$$\mathbf{H}^\varsigma = \sqrt{\sigma^\varsigma}\boldsymbol{\phi}^\varsigma\mathbf{V}^{\varsigma T}, \quad \mathbf{H}^\varsigma \in \mathbb{R}^{\delta \times \rho} \tag{5}$$

The regrouping of $\mathbf{H}^\varsigma|^{\varsigma=1,\ldots,d}$ into ξ linearly independent matrices terms $\mathbf{I}^j|^{j=1,\ldots,\xi}$, such that $\xi \leq d$, results in

$$\mathbf{H} = \mathbf{I}^1 + \mathbf{I}^2 + \cdots + \mathbf{I}^\xi \tag{6}$$

where ξ is the number of unobservable components extracted from experimental data. The unobservable spectral components $\alpha^j|^{j=1,\ldots,\xi}$ extracted from experimental data, resulted from the matrices $\mathbf{I}^j|^{j=1,\ldots,\xi}$, are given by:

$$\alpha_k^j = \begin{cases} \frac{1}{k}\sum_{\nu=1}^{k+1} I_{\nu,k-\nu+1}^j & 1 \leq k \leq \delta^* \\ \frac{1}{\delta^*}\sum_{\nu=1}^{\delta^*} I_{\nu,k-\nu+1}^j & \delta^* \leq k \leq \rho^* \\ \frac{1}{N_b-k+1}\sum_{\nu=k-\rho^*+1}^{N_b-\rho^*+1} I_{\nu,k-\nu+1}^j & \rho^* < k \leq N_b \end{cases} \tag{7}$$

where $\delta^* = \min(\delta, \rho)$, $\rho^* = \max(\delta, \rho)$ and $N_b = \delta + \rho - 1$.

3.1.2 Recursive step

After the initialization of spectral analysis algorithm in the training step, the next steps will be repeated for each time instant $k = N_b + 1, N_b + 2, \ldots$, as formulated in sequel. The value of ρ is increased by:

$$\rho = k - \delta + 1 \tag{8}$$

The covariance matrix is updated, recursively, as follows:

$$\mathbf{S}_k = \mathbf{S}_{k-1} + \boldsymbol{\Upsilon}_k, \qquad \mathbf{S}_k \in \mathbb{R}^{\delta \times \delta} \tag{9}$$

where $\boldsymbol{\Upsilon}_k = \boldsymbol{\psi}_k \boldsymbol{\psi}_k^T \in \mathbb{R}^{\delta \times \delta}$ with $\boldsymbol{\psi}_k = \left[y_\rho, y_{\rho+1}, \ldots, y_k\right]^T \in \mathbb{R}^{\delta \times 1}$. Applying SVD procedure to covariance matrix $\mathbf{S}_k$, the set of eigenvalues and their respective eigenvectors are updated such that the dynamic system output y_k can be rewritten by:

$$y_k = h_k^1 + h_k^2 + \cdots + h_k^d \tag{10}$$

where $h_k^\varsigma = \kappa_k^\varsigma \boldsymbol{\psi}_k^T \boldsymbol{\phi}_k^\varsigma$, with $\varsigma = 1, \ldots, d$, such that κ_k^ς corresponds to the last element of the eigenvector $\boldsymbol{\phi}_k^\varsigma$. Finally, the regrouping of the terms $h_k^\varsigma|^{\varsigma=1,\ldots,d}$ in ξ disjoint terms $I_k^j|^{j=1,\ldots,\xi}$, results in

$$y_k = I_k^1 + I_k^2 + \cdots + I_k^\xi \tag{11}$$

such that $I_k^j = \alpha_k^j$, with $j = 1, \ldots, \xi$ and $k = N_b + 1, N_b + 2, \ldots$, represents the samples of extracted unobservable components at instant k. The Recursive Singular Spectral Analysis, according to proposed methodology, is implemented as described in Algorithm 1.

3.1.3 Recursive estimation of measurement noise covariance

The spectral components, extracted by singular spectral analysis in Sect. 3.1, that presents smaller eigenvalues, are considered as residuals and they are used as data set for recursive estimation of measurement noise covariance R, inherited to experimental data. The initial covariance of measurement noise v, is given by:

$$R = \frac{1}{N_b} \sum_{j=1}^{N_b} v_j v_j^T \tag{12}$$

where N_b is the length of experimental data set to be used in training step for initial parameterization of interval type-2 fuzzy Kalman filter and v is the spectral component α^j considered as residual. The recursive updating of covariance R, at instants of time $k = N_b + 1, N_b + 2, \ldots$, is given by:

$$R_k = \frac{k-1}{k} R_{k-1} + \frac{1}{k} v_k v_k^T \tag{13}$$

Once the covariance R of the residual v is computed, an adaptive factor $\mathcal{X}_k$, with $k = N_b + 1, N_b + 2, \ldots$, is proposed, to be used as weighting factor for implementing the recursive updating mechanism of interval type-2 fuzzy Kalman filter, as follows:

$$\begin{cases} \mathcal{X}_k = 1 & \text{for} \quad R_k < 1 \\ \mathcal{X}_k = R_k^{-1} & \text{for} \quad 1 \leq R_k \leq 1000 \\ \mathcal{X}_k = 1 \times 10^{-3} & \text{for} \quad R_k > 1000 \end{cases} \tag{14}$$

Algorithm 1: Recursive Singular Spectral Analysis

input : $\mathbf{y}, \delta, \xi$

output: $\alpha_k^j|^{j=1,\ldots,\xi}$

%*Training step*;

Step 1: Compute $\rho = N_b - \delta + 1$;

Step 2: Construct the trajectory matrix $\mathbf{H}$ - Eq. (2);

Step 3: Compute the covariance matrix $\mathbf{S}$ - Eq. (3);

Step 4: Apply the SVD method in the covariance matrix $\mathbf{S}$;

Step 5: Compute $\mathbf{H}^\varsigma|^{\varsigma=1,\ldots,d}$ - Eq. (5) and obtain $\mathbf{I}^j|^{j=1,\ldots,\xi}$ - Eq. (6);

Step 6: Compute the unobservable components $\alpha_k^j|^{j=1,\ldots,\xi}$ - Eq. (7);

%*Recursive step*;

while $k \geq N_b + 1$ **do**

  Step 1: Update ρ - Eq. (8);

  Step 2: Update the covariance matrix $\mathbf{S}_k$ - Eq. (9);

  Step 3: Apply the SVD method in the covariance matrix $\mathbf{S}_k$;

  Step 4: Compute h_k^ς - Eq. (10) and obtain $I_k^j = \alpha_k^j|^{j=1,\ldots,\xi}$ - Eq. (11);

end

The algorithm for recursive estimation of noise covariance R and weighting factor $\mathcal{X}$, according to proposed methodology, is implemented as described in Algorithm 2.

Algorithm 2: Recursive Estimation of Measurement Noise Covariance and Weighting Factor

input : residual component α^j

output: $\mathcal{X}_k$, R_k

%*Training step*;

Compute R - Eq. (12) and $\mathcal{X}_k$ - Eq. (14);

%*Recursive step*;

while $k \geq N_b + 1$ **do**

  Update R_k - Eq. (13) and $\mathcal{X}_k$ - Eq. (14);

end

3.2 Parametric estimation of interval type-2 fuzzy Kalman filter

The adopted structure of interval type-2 fuzzy Kalman filter presents the $i|^{[i=1,2,\ldots,c]}$-th fuzzy rule, given by:

$$R^{(i)} : \text{IF } \mathbf{Z}_k \text{ IS } \widetilde{W}^i \quad \text{THEN} \begin{cases} \widetilde{\hat{\mathbf{x}}}_{k+1}^i = \widetilde{\mathbf{A}}_k^i \widetilde{\hat{\mathbf{x}}}_k^i + \widetilde{\mathbf{B}}_k^i \mathbf{u}_k + \boldsymbol{\mathcal{X}}_k \widetilde{\mathbf{K}}_k^i \widetilde{\boldsymbol{\epsilon}}_k^i \\ \widetilde{\hat{\mathbf{y}}}_k^i = \widetilde{\mathbf{C}}_k^i \widetilde{\hat{\mathbf{x}}}_k^i + \widetilde{\mathbf{D}}_k^i \mathbf{u}_k \end{cases} \tag{15}$$

with n-th order, m inputs, p outputs, where $\mathbf{Z}_k$ is the linguistic variable of the antecedent; $\widetilde{W}^i$ is the interval type-2 fuzzy set; $\widetilde{\hat{\mathbf{x}}}_k^i \in \mathbb{R}^n$ is the estimated interval states vector of the nonlinear dynamic system; $\widetilde{\hat{\mathbf{y}}}_k^i \in \mathbb{R}^p$ is the estimated interval output vector and $\mathbf{u}_k \in \mathbb{R}^m$ is the input signal. The matrices $\widetilde{\mathbf{A}}_k^i \in \mathbb{R}^{n\times n}$, $\widetilde{\mathbf{B}}_k^i \in \mathbb{R}^{n\times m}$, $\widetilde{\mathbf{C}}_k^i \in \mathbb{R}^{p\times n}$, $\widetilde{\mathbf{D}}_k^i \in \mathbb{R}^{p\times m}$ and $\widetilde{\mathbf{K}}_k^i \in \mathbb{R}^{n\times p}$ are, respectively, state matrix, input matrix, output matrix, direct transmission matrix and Kalman gain matrix, which are uncertain parameters that describe the dynamics of the nonlinear system within a region of uncertainty. The residual error $\widetilde{\boldsymbol{\epsilon}}_k^i$ for i-th rule is defined as $\widetilde{\boldsymbol{\epsilon}}_k^i = \mathbf{y}_k - \widetilde{\hat{\mathbf{y}}}_k^i$, where $\mathbf{y}_k \in \mathbb{R}^p$ is the real output of the dynamic system and $\widetilde{\hat{\mathbf{y}}}_k^i$ is the interval estimated output by i-th linear submodel, and the $\boldsymbol{\mathcal{X}}_k$ is the weighting factor, as formulated in Sect. 3.1.3, which corresponding to the level of filtering to be applied by interval type-2 fuzzy Kalman filter on the experimental data.

The interval type-2 fuzzy Kalman filter approximates the dynamic behavior inherited to experimental data through the weighted sum of Kalman filters defined in the consequent proposition of type-2 fuzzy Kalman filter rules, according to normalized interval activation degrees $\widetilde{\mu}_{\widetilde{W}^i}^i(\mathbf{Z}_k)$, of each i-th rule, as follows:

$$\begin{aligned} \widetilde{\hat{\mathbf{x}}}_{k+1} &= \sum_{i=1}^{c} \widetilde{\mu}_{\widetilde{W}^i}^i(\mathbf{Z}_k) \widetilde{\mathbf{A}}_k^i \widetilde{\hat{\mathbf{x}}}_k + \sum_{i=1}^{c} \widetilde{\mu}_{\widetilde{W}^i}^i(\mathbf{Z}_k) \widetilde{\mathbf{B}}_k^i \mathbf{u}_k \\ &\quad + \sum_{i=1}^{c} \widetilde{\mu}_{\widetilde{W}^i}^i(\mathbf{Z}_k) \boldsymbol{\mathcal{X}}_k \widetilde{\mathbf{K}}_k^i \widetilde{\boldsymbol{\epsilon}}_k^i \\ \widetilde{\hat{\mathbf{y}}}_k &= \sum_{i=1}^{c} \widetilde{\mu}_{\widetilde{W}^i}^i(\mathbf{Z}_k) \widetilde{\mathbf{C}}_k^i \widetilde{\hat{\mathbf{x}}}_k + \sum_{i=1}^{c} \widetilde{\mu}_{\widetilde{W}^i}^i(\mathbf{Z}_k) \widetilde{\mathbf{D}}_k^i \mathbf{u}_k \end{aligned} \tag{16}$$

with $\widetilde{\mu}_{\widetilde{W}^i}^i(\mathbf{Z}_k) = \left[\underline{\mu}_{\widetilde{W}^i}^i(\mathbf{Z}_k), \overline{\mu}_{\widetilde{W}^i}^i(\mathbf{Z}_k)\right]$, where $\underline{\mu}_{\widetilde{W}^i}^i(\mathbf{Z}_k)$ and $\overline{\mu}_{\widetilde{W}^i}^i(\mathbf{Z}_k)$ corresponds to lower and upper activation degrees in i-th cluster, respectively, and c is the number of rules of interval type-2 fuzzy Kalman filter, such that:

$$\sum_{i=1}^{c} \widetilde{\mu}_{\widetilde{W}^i}^i(\mathbf{Z}_k) = 1, \qquad \widetilde{\mu}_{\widetilde{W}^i}^i(\mathbf{Z}_k) \geq 0 \tag{17}$$

3.2.1 Parametric estimation of antecedent

The partitioning of experimental data implies to computing of operating regions and, necessarily, the number of rules of the interval type-2 fuzzy Kalman filter. An interval type-2 fuzzy version of Gustafson-Kessel clustering algorithm (Babuska 1998), was proposed, which is formulated in the sequel.

Given the experimental data set $\mathbf{Z}$, previously collected, choose the number of clusters $1 < c < N_b$; the random initial interval partition matrix $\widetilde{\mathbf{U}}^{(0)} \in \mathbb{R}^{c\times N_b}$, the termination tolerance $\mathcal{E} > 0$ and the interval weighting exponent $\widetilde{m} = [\underline{m}, \overline{m}]$, where $\underline{m}$ and $\overline{m}$ correspond to, respectively, weighting

exponent of upper and lower membership functions of the interval type-2 fuzzy set $\widetilde{W}^i$.

Repeat for $l = 1, 2, \ldots$

Step 1. Compute the centers of the clusters $\widetilde{\mathbf{v}}^{i(l)}$:

$$\widetilde{\mathbf{v}}^{i(l)} = \frac{\sum_{k=1}^{N_b} \left(\widetilde{\mu}^i_{\widetilde{W}^i}(\mathbf{Z}_k)^{i(l-1)}\right)^{\widetilde{m}} \mathbf{Z}_k}{\sum_{k=1}^{N_b} \left(\widetilde{\mu}^i_{\widetilde{W}^i}(\mathbf{Z}_k)^{(l-1)}\right)^{\widetilde{m}}}, \quad 1 \le i \le c \tag{18}$$

where $\mathbf{Z}_k$ is the data at sample k and $\widetilde{\mu}^i_{\widetilde{W}^i}(\mathbf{Z}_k)$ is the interval membership degree of $\mathbf{Z}_k$ in the i-th cluster.

Step 2. Compute the covariance matrices $\widetilde{\mathbf{F}}^i$ of the clusters:

$$\widetilde{\mathbf{F}}^i = \frac{\sum_{k=1}^{N_b} \left(\widetilde{\mu}^i_{\widetilde{W}^i}(\mathbf{Z}_k)^{(l-1)}\right)^{\widetilde{m}} \left(\mathbf{Z}_k - \widetilde{\mathbf{v}}^{i(l)}\right)\left(\mathbf{Z}_k - \widetilde{\mathbf{v}}^{i(l)}\right)^T}{\sum_{k=1}^{N} \left(\widetilde{\mu}^i_{\widetilde{W}^i}(\mathbf{Z}_k)^{(l-1)}\right)^{\widetilde{m}}}, \quad 1 \le i \le c, \;\; 1 \le k \le N_b \tag{19}$$

Step 3. Compute the distances $\widetilde{D}^i_{k\widetilde{\mathbf{F}}^i}$:

$$\widetilde{D}^i_{k\widetilde{\mathbf{F}}^i} = \sqrt{\left(\mathbf{Z}_k - \widetilde{\mathbf{v}}^{i(l)}\right)^T \left[\det\left(\widetilde{\mathbf{F}}^i\right)^{1/n} \left(\widetilde{\mathbf{F}}^i\right)^{-1}\right] \left(\mathbf{Z}_k - \widetilde{\mathbf{v}}^{i(l)}\right)} \tag{20}$$

Step 4. Update the partition matrix $\widetilde{\mathbf{U}}^{(l)}$:

If $\widetilde{D}^i_{k\widetilde{\mathbf{F}}^i} > 0$ for $1 \le i \le c, 1 \le k \le N_b$

$$\widetilde{\mu}^{i(l)}_{\widetilde{W}^i}(\mathbf{Z}_k) = \left[\underline{\mu}^i_{\widetilde{W}^i}(\mathbf{Z}_k), \overline{\mu}^i_{\widetilde{W}^i}(\mathbf{Z}_k)\right] \tag{21}$$

where

$$\underline{\mu}^{i(l)}_{\widetilde{W}^i}(\mathbf{Z}_k) = \min\left[\frac{1}{\sum_{j=1}^{c}\left(\underline{D}^i_{k\underline{\mathbf{F}}^i}/\underline{D}^i_{k\underline{\mathbf{F}}^i}\right)^{2/(\underline{m}-1)}}, \; \frac{1}{\sum_{j=1}^{c}\left(\overline{D}^i_{k\overline{\mathbf{F}}^i}/\overline{D}^i_{k\overline{\mathbf{F}}^i}\right)^{2/(\overline{m}-1)}}\right] \tag{22}$$

$$\overline{\mu}^{i(l)}_{\widetilde{W}^i}(\mathbf{Z}_k) = \max\left[\frac{1}{\sum_{j=1}^{c}\left(\underline{D}^i_{k\underline{\mathbf{F}}^i}/\underline{D}^i_{k\underline{\mathbf{F}}^i}\right)^{2/(\underline{m}-1)}}, \; \frac{1}{\sum_{j=1}^{c}\left(\overline{D}^i_{k\overline{\mathbf{F}}^i}/\overline{D}^i_{k\overline{\mathbf{F}}^i}\right)^{2/(\overline{m}-1)}}\right] \tag{23}$$

otherwise

$\widetilde{\mu}^{i(l)}_{\widetilde{W}^i}(\mathbf{Z}_k) = [0,\ 0]$ with $\underline{\mu}^{i(l)}_{\widetilde{W}^i}(\mathbf{Z}_k) \in [0,1]$ e $\overline{\mu}^{i(l)}_{\widetilde{W}^i}(\mathbf{Z}_k) \in [0,1]$

Until $\left\|\widetilde{\mathbf{U}}^{(l)} - \widetilde{\mathbf{U}}^{(l-1)}\right\| < \mathcal{E}$

The interval type-2 fuzzy Gustafson-Kessel clustering algorithm, according to proposed methodology, is implemented as described in Algorithm 3.

Algorithm 3: Interval Type-2 Fuzzy Gustafson-Kessel Clustering Algorithm

input : $\mathbf{Z}, \widetilde{m}, \mathcal{E}, \widetilde{\mathbf{U}}^{(0)}$
output: $\widetilde{\mathbf{U}}$
$l = 0$;
repeat
  $l = l + 1$;
  for $i = 1$ **to** c **do**
    Step 1: Compute the centers of the clusters $\widetilde{\mathbf{v}}^{i(l)}$ - Eq. (18);
    Step 2: Compute the covariance matrices of the clusters $\widetilde{\mathbf{F}}^i$ - Eq. (19);
    Step 3 - Compute the distances $\widetilde{D}^i_{k\widetilde{\mathbf{F}}^i}$ - Eq. (20);
    Step 4: Update the partition matrix $\widetilde{\mathbf{U}}^{(l)}$ - Eq. (21)-(23);
  end
until $\left\|\widetilde{\mathbf{U}}^{(l)} - \widetilde{\mathbf{U}}^{(l-1)}\right\| < \mathcal{E}$;

3.2.2 Parametric estimation of consequent

The interval type-2 fuzzy OKID (Observer/Kalman Filter Identification) algorithm, is proposed, as formulated in the sequel. Let the experimental dataset $\mathbf{Z}$, such that $\mathbf{Z}_k = \left[\mathbf{u}_k \boldsymbol{\alpha}_k^*\right]^T$, where $\boldsymbol{\alpha}_k^*$ corresponds to spectral components extracted from the experimental dataset that presents higher eigenvalue and are more significant to represent the dynamics of experimental dataset. Choose an appropriate number of Markov parameters q, through the following steps:

Step 1. Compute the matrix of regressors $\boldsymbol{\Lambda}$, given by:

$$\boldsymbol{\Lambda} = \begin{bmatrix} \mathbf{u}_q & \mathbf{u}_{q+1} & \cdots & \mathbf{u}_{N_b-1} \\ \mathbf{Z}_{q-1} & \mathbf{Z}_q & \cdots & \mathbf{Z}_{N_b-2} \\ \mathbf{Z}_{q-2} & \mathbf{Z}_{q-1} & \cdots & \mathbf{Z}_{N_b-3} \\ \vdots & \vdots & \ddots & \vdots \\ \mathbf{Z}_0 & \mathbf{Z}_1 & \cdots & \mathbf{Z}_{N_b-q-1} \end{bmatrix} \tag{24}$$

Step 2. Compute the interval observer Markov parameters $\widetilde{\overline{\mathbf{Y}}}^i$:

$$\widetilde{\hat{\mathbf{y}}}^T = \sum_{i=1}^{c} \widetilde{\boldsymbol{\Gamma}}^i \boldsymbol{\Lambda}^T \widetilde{\overline{\mathbf{Y}}}^{i^T} \tag{25}$$

where

$$\widetilde{\boldsymbol{\Gamma}}^i = \begin{bmatrix} \widetilde{\mu}^i_{\widetilde{W}^i}(\mathbf{Z}_q) & 0 & \ldots & 0 \\ 0 & \widetilde{\mu}^i_{\widetilde{W}^i}(\mathbf{Z}_{q+1}) & \ldots & 0 \\ 0 & 0 & \ldots & 0 \\ \vdots & \vdots & \ddots & \vdots \\ 0 & 0 & \ldots & \widetilde{\mu}^i_{\widetilde{W}^i}(\mathbf{Z}_{N_b-1}) \end{bmatrix} \tag{26}$$

is the diagonal weighting matrix of the i-th fuzzy rule obtained from the interval type-2 Gustafson-Kessel fuzzy clustering algorithm and

$$\begin{aligned} \widetilde{\overline{\mathbf{Y}}}^i &= \left[\widetilde{\mathbf{D}}^i_k \;\; \widetilde{\mathbf{C}}^i_k \widetilde{\overline{\mathbf{B}}}^i_k \;\; \widetilde{\mathbf{C}}^i_k \widetilde{\overline{\mathbf{A}}}^i_k \widetilde{\overline{\mathbf{B}}}^i_k \;\; \cdots \;\; \widetilde{\mathbf{C}}^i_k \widetilde{\overline{\mathbf{A}}}^{i^{(q-1)}}_k \widetilde{\overline{\mathbf{B}}}^i_k \right] \\ &= \left[\widetilde{\overline{\mathbf{Y}}}_0 \;\; \widetilde{\overline{\mathbf{Y}}}_1 \;\; \widetilde{\overline{\mathbf{Y}}}_2 \;\; \cdots \widetilde{\overline{\mathbf{Y}}}_q \right] \end{aligned} \tag{27}$$

is the interval observer Markov parameters of i-th rule such that

$$\widetilde{\overline{\mathbf{A}}}^i_k = \left[\widetilde{\mathbf{A}}^i_k + \widetilde{\mathbf{K}}^i_k \widetilde{\mathbf{C}}^i_k \right] \tag{28}$$

$$\widetilde{\overline{\mathbf{B}}}^i_k = \left[\widetilde{\mathbf{B}}^i_k + \widetilde{\mathbf{K}}^i_k \widetilde{\mathbf{D}}^i_k \;, -\widetilde{\mathbf{K}}^i_k \right] \tag{29}$$

and $\widetilde{\hat{\mathbf{y}}}$ is the interval output of type-2 fuzzy Kalman filter.

Manipulating the Eq. (25):

$$\boldsymbol{\Lambda} \widetilde{\boldsymbol{\Gamma}}^i \mathbf{y}^T = \boldsymbol{\Lambda} \widetilde{\boldsymbol{\Gamma}}^i \boldsymbol{\Lambda}^T \widetilde{\overline{\mathbf{Y}}}^{i^T} \tag{30}$$

where $\mathbf{y} = \begin{bmatrix} \mathbf{y}_1 & \mathbf{y}_2 & \ldots & \mathbf{y}_{N_b} \end{bmatrix} \in \mathbb{R}^{p \times N_b}$ corresponds to output vector of dynamic system. Assuming $\widetilde{\mathfrak{U}}^i = \boldsymbol{\Lambda} \widetilde{\boldsymbol{\Gamma}}^i \boldsymbol{\Lambda}^T$ and $\widetilde{\aleph}^i = \boldsymbol{\Lambda} \widetilde{\boldsymbol{\Gamma}}^i \mathbf{y}^T$, Eq. (30) is rewriting as:

$$\widetilde{\mathfrak{U}}^i \widetilde{\overline{\mathbf{Y}}}^{i^T} = \widetilde{\aleph}^i \tag{31}$$

The Eq. (31) is solved by QR factorization method (Chen 1999), which is numerically robust since it avoids matrix inverse operations. Applying QR factorization to the term $\widetilde{\mathfrak{U}}^i$ on the right side of the Eq. (31), it has:

$$\widetilde{\mathbf{Q}}^i \widetilde{\mathbf{R}}^i \widetilde{\overline{\mathbf{Y}}}^{i^T} = \widetilde{\aleph}^i \tag{32}$$

where $\widetilde{\mathbf{Q}}^i$ is an orthogonal matrix, such that $\left(\widetilde{\mathbf{Q}}^i\right)^{-1} = \left(\widetilde{\mathbf{Q}}^i\right)^T$ and $\widetilde{\mathbf{R}}^i$ is an upper triangular matrix. Because the matrix $\widetilde{\mathbf{R}}^i$ is upper triangular, Eq. (32) can be solved by backward replacement, obtaining the observer's Markov parameter vector $\widetilde{\overline{\mathbf{Y}}}^i$.

Step 3. Compute the observer gain and system Markov parameters:

$$\widetilde{\overline{\mathbf{Y}}}^i_0 = \widetilde{\mathbf{D}}^i_k \tag{33}$$

$$\widetilde{\overline{\mathbf{Y}}}^i_j = \widetilde{\mathbf{C}}^i_k \widetilde{\overline{\mathbf{A}}}^{i^{(j-1)}}_k \widetilde{\overline{\mathbf{B}}}^i_k \tag{34}$$

$$\begin{aligned} &= \left[\widetilde{\mathbf{C}}^i_k \left(\widetilde{\mathbf{A}}^i_k + \widetilde{\mathbf{K}}^i_k \widetilde{\mathbf{C}}^i_k \right)^{(j-1)} \left(\widetilde{\mathbf{B}}^i_k + \widetilde{\mathbf{K}}^i_k \widetilde{\mathbf{D}}^i_k \right), \right. \\ &\quad \left. -\widetilde{\mathbf{C}}^i_k \left(\widetilde{\mathbf{A}}^i_k + \widetilde{\mathbf{K}}^i_k \widetilde{\mathbf{C}}^i_k \right)^{(j-1)} \widetilde{\mathbf{K}}^i_k \right] \end{aligned} \tag{35}$$

$$= \left[\widetilde{\overline{\mathbf{Y}}}^{i^{(1)}}_j \;, \; -\widetilde{\overline{\mathbf{Y}}}^{i^{(2)}}_j \right], \; j = 1, 2, 3, \ldots \tag{36}$$

where $\widetilde{\overline{\mathbf{Y}}}^i_j$ are the interval observer Markov parameters obtained from Step 2 for i-th cluster. Thus, the system Markov parameters $\widetilde{\mathbf{Y}}^i_j$ are obtained as follows:

$$\widetilde{\mathbf{Y}}^i_0 = \widetilde{\overline{\mathbf{Y}}}^i_0 = \widetilde{\mathbf{D}}^i_k \tag{37}$$

$$\widetilde{\mathbf{Y}}^i_j = \widetilde{\overline{\mathbf{Y}}}^{i^{(1)}}_j - \sum_{\iota=1}^{j} \widetilde{\overline{\mathbf{Y}}}^{i^{(2)}}_j \widetilde{\mathbf{Y}}^i_{j-\iota}, \text{ for } j = 1, \ldots, q \tag{38}$$

$$\widetilde{\mathbf{Y}}_j^i = -\sum_{\iota=1}^{q} \widetilde{\overline{\mathbf{Y}}}_j^{i^{(2)}} \widetilde{\mathbf{Y}}_{j-\iota}^i, \text{ for } j = q+1, \ldots, \infty \tag{39}$$

and the observer gain Markov parameters $\widetilde{\mathbf{Y}}_j^{i^o}$ are obtained by:

$$\widetilde{\mathbf{Y}}_1^{i^o} = \widetilde{\overline{\mathbf{Y}}}_1^{i^{(2)}} = \widetilde{\mathbf{C}}_k^i \widetilde{\mathbf{K}}_k^i \tag{40}$$

$$\widetilde{\mathbf{Y}}_j^{i^o} = \widetilde{\overline{\mathbf{Y}}}_j^{i^{(2)}} - \sum_{\iota=1}^{j-1} \widetilde{\overline{\mathbf{Y}}}_j^{i^{(2)}} \widetilde{\mathbf{Y}}_{j-\iota}^{i^o}, \text{ for } j = 2, \ldots, q \tag{41}$$

$$\widetilde{\mathbf{Y}}_j^{i^o} = -\sum_{\iota=1}^{q} \widetilde{\overline{\mathbf{Y}}}_j^{i^{(2)}} \widetilde{\mathbf{Y}}_{j-\iota}^{i^o}, \text{ for } j = q+1, \ldots, \infty \tag{42}$$

Step 4. **Step 4** - Construct the Hankel matrix $\widetilde{\mathbf{H}}^i(j-1) \in \mathbb{R}^{\gamma p \times \beta m}$:

$$\widetilde{\mathbf{H}}^i(j-1) = \begin{bmatrix} \widetilde{\mathbf{Y}}_j^i & \widetilde{\mathbf{Y}}_{j+1}^i & \cdots & \widetilde{\mathbf{Y}}_{j+\beta-1}^i \\ \widetilde{\mathbf{Y}}_{j+1}^i & \widetilde{\mathbf{Y}}_{j+2}^i & \cdots & \widetilde{\mathbf{Y}}_{j+\beta}^i \\ \vdots & \vdots & \ddots & \vdots \\ \widetilde{\mathbf{Y}}_{j+\gamma-1}^i & \widetilde{\mathbf{Y}}_{j+\gamma}^i & \cdots & \widetilde{\mathbf{Y}}_{j+\gamma+\beta-2}^i \end{bmatrix} \tag{43}$$

where γ and β are sufficiently large arbitrary integers defined by user.

Step 5. For $j = 1$, decompose $\widetilde{\mathbf{H}}^i(0)$ using Singular Value Decomposition:

$$\widetilde{\mathbf{H}}^i(0) = \widetilde{\mathbf{\Xi}}^i \widetilde{\mathbf{\Sigma}}^i \widetilde{\mathbf{\Psi}}^{i^T} \tag{44}$$

where $\widetilde{\mathbf{\Xi}}^i \in \mathbb{R}^{\alpha p \times \alpha p}$ and $\widetilde{\mathbf{\Psi}}^i \in \mathbb{R}^{\beta m \times \beta m}$ are orthogonal matrices and $\widetilde{\mathbf{\Sigma}}^i \in \mathbb{R}^{\alpha p \times \beta m}$ is the diagonal matrix of singular values defined as:

$$\widetilde{\mathbf{\Sigma}}^i = \begin{bmatrix} \widetilde{\mathbf{\Sigma}}_n^i & 0 \\ 0 & 0 \end{bmatrix} \tag{45}$$

such that n is the number of significant singular values and determines the minimum order of the type-2 fuzzy Kalman filter. Thus, the size of matrices in Eq. (44) is reduced to the minimum order, as follows:

$$\widetilde{\mathbf{H}}_n^i(0) = \widetilde{\mathbf{\Xi}}_n^i \widetilde{\mathbf{\Sigma}}_n^i \widetilde{\mathbf{\Psi}}_n^{i^T} \tag{46}$$

where $\widetilde{\mathbf{\Xi}}_n^i \in \mathbb{R}^{\alpha p \times n}$, $\widetilde{\mathbf{\Psi}}_n^i \in \mathbb{R}^{\beta m \times n}$, $\widetilde{\mathbf{\Sigma}}_n^i \in \mathbb{R}^{n \times n}$ are the resulting matrices after the reduction to minimum order.

Step 6. Compute the observability and controllability matrices:

$$\widetilde{\mathcal{P}}_\gamma^i = \widetilde{\mathbf{\Xi}}_n^i \left(\widetilde{\mathbf{\Sigma}}_n^i\right)^{1/2} \tag{47}$$

$$\widetilde{\mathcal{Q}}_\beta^i = \left(\widetilde{\mathbf{\Sigma}}_n^i\right)^{1/2} \widetilde{\mathbf{\Psi}}_n^{i^T} \tag{48}$$

where

$$\widetilde{\mathcal{P}}_\gamma^i = \begin{bmatrix} \widetilde{\mathbf{C}}_k^i \\ \widetilde{\mathbf{C}}_k^i \widetilde{\mathbf{A}}_k^i \\ \widetilde{\mathbf{C}}_k^i \widetilde{\mathbf{A}}_k^{i^2} \\ \vdots \\ \widetilde{\mathbf{C}}_k^i \widetilde{\mathbf{A}}_k^{i^{\gamma-1}} \end{bmatrix} \tag{49}$$

is the observability matrix and

$$\widetilde{\mathcal{Q}}_\beta^i = \begin{bmatrix} \widetilde{\mathbf{B}}_k^i & \widetilde{\mathbf{A}}_k^i \widetilde{\mathbf{B}}_k^i & \widetilde{\mathbf{A}}_k^{i^2} \widetilde{\mathbf{B}}_k^i & \cdots & \widetilde{\mathbf{A}}_k^{i^{\beta-1}} \widetilde{\mathbf{B}}_k^i \end{bmatrix} \tag{50}$$

is the controllability matrix.

Step 7. Compute the matrices that make up the consequent proposition of interval type-2 fuzzy Kalman filter:

$$\widetilde{\mathbf{A}}_k^i = \left(\widetilde{\mathbf{\Sigma}}_n^i\right)^{-1/2} \widetilde{\mathbf{\Xi}}_n^{i^T} \widetilde{\mathbf{H}}_n^i(1) \widetilde{\mathbf{\Psi}}_n^{i^T} \left(\widetilde{\mathbf{\Sigma}}_n^i\right)^{-1/2} \tag{51}$$

$$\widetilde{\mathbf{B}}_k^i = \text{first } m \text{ collumns of } \mathcal{Q}_\beta^i \tag{52}$$

$$\widetilde{\mathbf{C}}_k^i = \text{first } p \text{ rows of } \mathcal{P}_\beta^i \tag{53}$$

$$\widetilde{\mathbf{D}}_k^i = \widetilde{\mathbf{Y}}_0^i \tag{54}$$

Step 8. Compute the interval Kalman gain matrix:

$$\widetilde{\mathbf{Y}}_j^{i^o} = -\widetilde{\mathcal{P}}_\beta^i \widetilde{\mathbf{K}}_k^i \tag{55}$$

where $\widetilde{\mathbf{Y}}_j^{i^o}$ is the observer gain Markov parameters, $\widetilde{\mathcal{P}}_\beta^i$ is the observability matrix and $\widetilde{\mathbf{K}}_k^i$ is the interval Kalman gain matrix. Manipulating the Eq. (55):

$$\widetilde{\mathcal{P}}_\beta^{i^T} \widetilde{\mathbf{\Gamma}}^i \widetilde{\mathbf{Y}}_j^{i^o} = -\widetilde{\mathcal{P}}_\beta^{i^T} \widetilde{\mathbf{\Gamma}}^i \widetilde{\mathcal{P}}_\beta^i \widetilde{\mathbf{K}}_k^i \tag{56}$$

Assuming $\widetilde{\mathfrak{A}}^i = -\widetilde{\mathcal{P}}_\beta^{i^T} \widetilde{\mathbf{\Gamma}}^i \widetilde{\mathcal{P}}_\beta^i$ and $\widetilde{\mathfrak{N}}^i = \widetilde{\mathcal{P}}_\beta^{i^T} \widetilde{\mathbf{\Gamma}}^i \widetilde{\mathbf{Y}}_j^{i^o}$, Eq. (56) is rewriting as follows:

$$\widetilde{\mathfrak{A}}^i \widetilde{\mathbf{K}}_k^i = \widetilde{\mathfrak{N}}^i \tag{57}$$

The Eq. (57) is solved by QR factorization method being applied to $\widetilde{\mathfrak{A}}^i$ and obtaining the interval Kalman gain matrix $\widetilde{\mathbf{K}}_k^i$ in the same way as done in Step 2 for determining interval observer Markov parameters.

Recursive updating of interval type-2 fuzzy Kalman filter inference system After the initial estimation of interval type-2 fuzzy Kalman filter, the Kalman filters, into consequent proposition of interval type-2 fuzzy Kalman filter inference system, are updated recursively at instants of time $k = N_b + 1, k = N_b + 2, \ldots$, to each new sample from experimental data set. Considering the regressors vector $\boldsymbol{\lambda}_k$, at instant k, given by

$$\boldsymbol{\lambda}_k = \begin{bmatrix} \mathbf{u}_{k+1} \\ \mathbf{Z}_k \\ \mathbf{Z}_{k-1} \\ \vdots \\ \mathbf{Z}_{k-q} \end{bmatrix} \tag{58}$$

the interval observer Markov parameters $\widetilde{\overline{\mathbf{Y}}}_k^i$ are obtained by recursive updating of Eq. (31), as follows:

$$\widetilde{\mathfrak{U}}_k^i = \widetilde{\mathfrak{U}}_{k-1}^i + \widetilde{\mu}_{\widetilde{W}^i}^i(\mathbf{Z}_k)\boldsymbol{\lambda}_k\boldsymbol{\lambda}_k^T \tag{59}$$

$$\widetilde{\mathfrak{K}}_k^i = \widetilde{\mathfrak{K}}_{k-1}^i + \widetilde{\mu}_{\widetilde{W}^i}^i(\mathbf{Z}_k)\boldsymbol{\lambda}_k\mathbf{y}_k^T \tag{60}$$

Once $\widetilde{\mathfrak{U}}_k^i$ and $\widetilde{\mathfrak{K}}_k^i$ have been updated, and applying the QR factorization in $\widetilde{\mathfrak{U}}_k^i$, the observer Markov parameters for i-th cluster at sample k, $\widetilde{\overline{\mathbf{Y}}}_k^i$, are updated. The consequent proposition of the type-2 fuzzy Kalman filter is updated recursively by repeating the Steps 3–7. Similarly, the interval type-2 fuzzy Kalman gain matrix $\widetilde{\mathbf{K}}_k^i$ is obtained by recursive updating of Eq. (57), as follows:

$$\widetilde{\mathfrak{A}}_k^i = \widetilde{\mathfrak{A}}_{k-1}^i + \widetilde{\mu}_{\widetilde{W}^i}^i(\mathbf{Z}_k)\boldsymbol{\lambda}_k\boldsymbol{\lambda}_k^T \tag{61}$$

$$\widetilde{\mathfrak{N}}_k^i = \widetilde{\mathfrak{N}}_{k-1}^i + \widetilde{\mu}_{\widetilde{W}^i}^i(\mathbf{Z}_k)\boldsymbol{\lambda}_k\boldsymbol{\lambda}_k^T \tag{62}$$

Once $\widetilde{\mathfrak{A}}_k^i$ and $\widetilde{\mathfrak{N}}_k^i$ have been updated, and applying the QR factorization method in $\widetilde{\mathfrak{A}}_k^i$, the interval type-2 fuzzy Kalman gain matrix is updated.

The interval type-2 fuzzy Observer/Kalman Filter Identification algorithm, according to proposed methodology, is implemented as described in Algorithm 4.

Algorithm 4: Interval Type-2 Fuzzy Observer/Kalman Filter Identification Algorithm

input : $\mathbf{Z}, \gamma, \beta, q, \widetilde{\mathbf{\Gamma}}^i$
output: $\widetilde{\mathbf{A}}_k^i, \widetilde{\mathbf{B}}_k^i, \widetilde{\mathbf{C}}_k^i, \widetilde{\mathbf{D}}_k^i, \widetilde{\mathbf{K}}_k^i$
Step 1: Construct the matrix of regressors $\mathbf{\Lambda}$ - Eq. (24);
%*Training step*;
for $i = 1$ **to** c **do**
  Step 2: Compute the interval observer Markov parameters $\widetilde{\overline{\mathbf{Y}}}^i$ - Eq. (30)-(32);
  Step 3: Compute the interval system Markov parameters $\widetilde{\mathbf{Y}}^i$ - Eq. (37)-(39) and the interval observer gain Markov parameters $\widetilde{\mathbf{Y}}^{i^o}$ - Eq. (40)-(42) ;
  Step 4: Construct the Hankel matrices $\widetilde{\mathbf{H}}^i(0)$ and $\widetilde{\mathbf{H}}^i(1)$ - Eq. (43);
  Step 5: Decompose $\widetilde{\mathbf{H}}^i(0)$ using SVD method - Eq. (44) and determine the minimum order of realization n - Eq. (45);
  Step 6: Compute the observability matrix $\widetilde{\mathcal{P}}_\gamma^i$ - Eq. (47) and the controlability matrix $\widetilde{\mathcal{Q}}_\beta^i$ - Eq. (48);
  Step 7: Compute the matrices $\widetilde{\mathbf{A}}_k^i$, $\widetilde{\mathbf{B}}_k^i$, $\widetilde{\mathbf{C}}_k^i$, $\widetilde{\mathbf{D}}_k^i$ - Eq. (51)-(54);
  Step 8: Compute the interval Kalman gain matrix $\widetilde{\mathbf{K}}_k^i$ - Eq. (55)-(57);
end
%*Recursive update of interval type-2 fuzzy Kalman filter*;
while $k \geq N_b + 1$ **do**
  Construct the regressors vector $\boldsymbol{\lambda}_k$ - Eq. (58);
  for $i = 1$ **to** c **do**
    Update the interval Markov parameters - Eq. (59)-(60);
    Repeat **Step 3** to **Step 7** described in training step;
    Update the interval Kalman gain matrix - Eq. (61)-(62)
  end
end

3.3 Computational load analysis of interval type-2 fuzzy Kalman filter algorithm

The parameters γ, β and q must be adequately defined for implementation of interval type-2 fuzzy Kalman filter algorithm, that requires some intuition by expert on the experimental dataset. The parameters γ and β are related to dimension and rank of Hankel matrix in Eq. (43) so that a good conditioning can be guaranteed for parametric estimation of consequent proposition in interval type-2 fuzzy Kalman filter, according to Eqs. (51)–(54), whose most typical values are into the interval $\frac{N_b}{10} < \gamma, \beta < \frac{N_b}{2}$, where N_b is the length of experimental dataset (Juang 1994; Hangos et al. 2004). The numerical value of q is related to the number of observer's Markov parameters, i.e., the most representative factors of impulse response from experimental dataset, according to Eq. (27), so that $CA^kB \approx 0$ for $k \geq q$ implies to the truncated matrix $\widetilde{\overline{\mathbf{Y}}}^i$, in order to lead to a unique solution for the parametric estimation of consequent proposition in interval type-2 fuzzy Kalman filter, whose most typical values are into the interval $1 \leq q \leq 10$ (Callier and Desoer 1991; Antsaklis and Astolfi 2020).

The computational load of the interval type-2 fuzzy Kalman filter algorithm, in the each iteration, is related to the number of fuzzy rules and the number of estimated parameters, according as following:

$$CL = 2 \times c \times N_p \tag{63}$$

where CL is the computational load, c is the number of fuzzy rules and N_p is the number of parameters estimated by interval type-2 fuzzy Kalman filter, which are the matrices $\mathbf{A}, \mathbf{B}, \mathbf{C}, \mathbf{D}, \mathbf{K}$. The multiplicative factor 2 is applied as a consequence of the interval type-2 structure of the fuzzy Kalman filter algorithm, i. e., it is required the nonlinear combination of two groups of fuzzy Kalman filters to define the upper and lower limits for tracking and forecasting of experimental dataset.

Since the number of fuzzy rules c is pre-established and the interval type-2 fuzzy Kalman filter algorithm guarantees the minimum realization for the identified model, i. e, establishes the smallest possible order for the matrices $\mathbf{A}, \mathbf{B}, \mathbf{C}, \mathbf{D}, \mathbf{K}$, the computational load defined in Eq. (63) for the implementation of the proposed methodology is minimal.

4 Results

In this section, computational results from filtering and tracking the reference trajectory through state variables of a nonlinear dynamic system with chaotic behavior and time delays, are shown to illustrate the efficiency of proposed methodology as compared to other approaches widely cited in the literature. Experimental results from real time interval tracking and forecasting the COVID-19's dynamic spreading behavior in Brazil, so to demonstrate the applicability of proposed methodology, are also presented.

4.1 Computational results

In this section, computational results for filtering and tracking the reference trajectory through state variables of Chen's chaotic attractor in a noisy environment, is presented.

4.1.1 Interval type-2 fuzzy Kalman filtering and tracking of Chen's chaotic attractor

The Chen's chaotic attractor (1999), is given by:

$$\begin{aligned} \dot{x}_1 &= \eta(x_2 - x_1) \\ \dot{x}_2 &= (\vartheta - \eta)x_1 + bx_2 - x_1x_3 \\ \dot{x}_3 &= x_1x_2 - \hbar x_3 \end{aligned} \tag{64}$$

where the parameters $\eta = 35$, $\vartheta = 28$ and $\hbar = 3$ provide a chaotic behavior. A data set from Chen's chaotic attractor, considering the initial condition $\mathbf{x}_0 = [-10 \;\; 0 \;\; 37]^T$, with total length of 4000 samples by a sampling period of $T = 2,5\text{m}s$, was generated. A reference trajectory $\mathbf{r}(t)$ was constructed by artificially repeating some portion $\mathbf{x}(1696)$, $\mathbf{x}(1697)$, $\cdots$, $\mathbf{x}(1982)$ of the original data with a smoothly interpolated portion $\{\check{\mathbf{x}}(1983), \check{\mathbf{x}}(1984), \check{\mathbf{x}}(1985)\}$ obtained as follows (Wu et al. 2015):

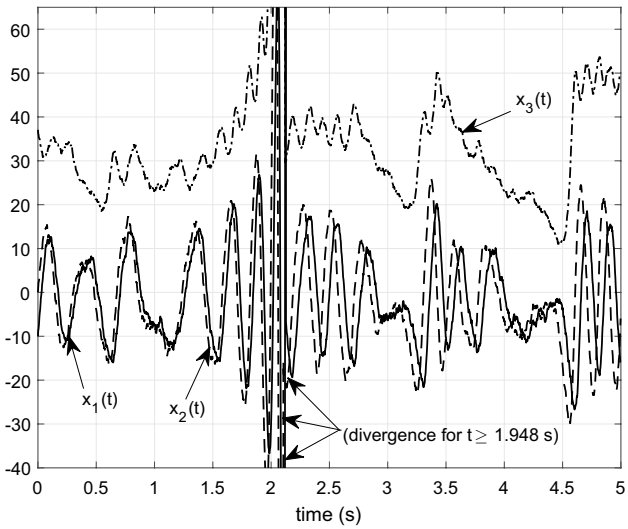

Fig. 1 Experimental data set of Chen's chaotic attractor with unexpected time-delays during $1,5\ s \leq t \leq 3,5\ s$

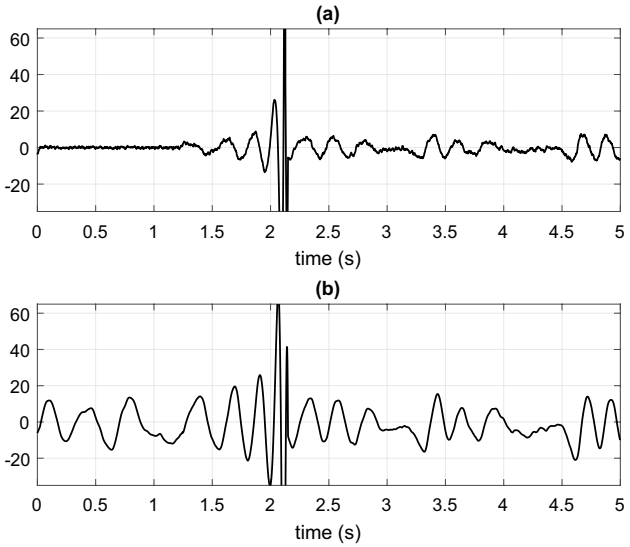

Fig. 2 The spectral components $\alpha^j|^{j=1,\ldots,2}$, which were extracted for state variable x_1 from Chen's chaotic attractor: **a** α^1; **b** α^2

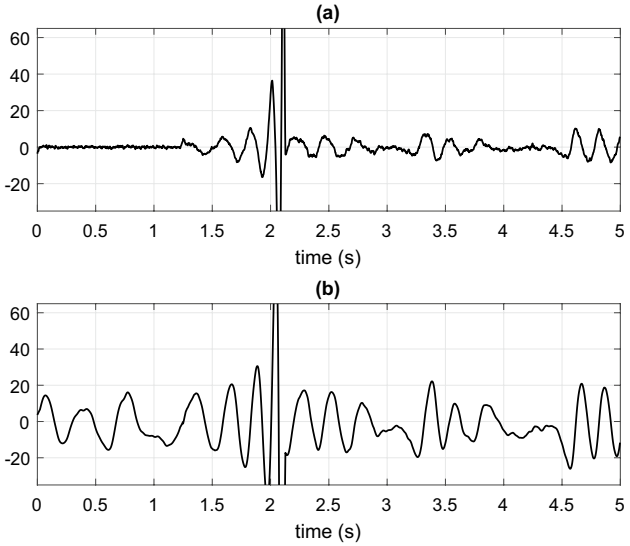

Fig. 3 The spectral components $\alpha^j|^{j=1,\ldots,2}$, which were extracted for state variable x_2 from Chen's chaotic attractor: **a** α^1; **b** α^2

$$\check{\mathbf{x}}(1982+\omega)=\mathbf{x}(1982)+\frac{\omega}{4}[\mathbf{x}(1696)-\mathbf{x}(1982)] \tag{65}$$

with $\omega=1,2,\ldots,N-1$ ($N=4$ for this experiment), such that the reference trajectory $\mathbf{r}(t)=\left[r_1(t)\ \ r_2(t)\ \ r_3(t)\right]^T$ must be tracked by state variables of Chen's chaotic attractor. The variable $\mathbf{u}_k$, in Eq. 15 of proposed methodology, is considered as white noise signal with variance of each input given by (Wu et al. 2015):

$$\sigma(u_{\mathcal{M}}(t))=0.5\%\times\left[\max r_{\mathcal{M}}(kT)-\min r_{\mathcal{M}}(kT)\right],\ \ \mathcal{M}=1,\ldots,3 \tag{66}$$

resulting in

$$\sigma(\mathbf{u}(t))=[0.129\ \ 0.135\ \ 0.055]^T \tag{67}$$

where $\mathbf{u}(t)=\left[u_1(t)\ \ u_2(t)\ \ u_3(t)\right]^T$ is the input vector applied to Chen's chaotic attractor dynamic system. In the application context of interval type-2 fuzzy Kalman filter for tracking the reference trajectory $\mathbf{r}(t)$, the occurrence of unexpected time-delays in inputs and states is considered, such that the Chen's chaotic attractor dynamic system is described by:

$$\begin{bmatrix}\dot{x}_1(t)\\ \dot{x}_2(t)\\ \dot{x}_3(t)\end{bmatrix}=\begin{bmatrix}-\eta & \eta & 0\\ \vartheta-\eta & \vartheta & 0\\ 0 & 0 & -\hbar\end{bmatrix}\begin{bmatrix}x_1(t-\tau_1)\\ x_2(t-\tau_2)\\ x_3(t-\tau_3)\end{bmatrix}+\begin{bmatrix}0\\ x_1(t-\tau_1)x_3(t-\tau_3)\\ x_1(t-\tau_1)x_2(t-\tau_2)\end{bmatrix}+\begin{bmatrix}u_1(t-\tau_4)\\ u_2(t-\tau_5)\\ u_3(t-\tau_6)\end{bmatrix}+w(t) \tag{68}$$

$$\begin{bmatrix}y_1(t)\\ y_2(t)\\ y_3(t)\end{bmatrix}=\begin{bmatrix}1 & 0 & 0\\ 0 & 1 & 0\\ 0 & 0 & 1\end{bmatrix}\begin{bmatrix}x_1(t-\tau_1)\\ x_2(t-\tau_2)\\ x_3(t-\tau_3)\end{bmatrix}+v(t) \tag{69}$$

where $w(t)$ and $v(t)$ are, respectively, zero-mean white noises of process and measurement such that the covariances are defined as cov $(w)=0,02$ and cov $(v)=0,002$. The state time-delays are $\tau_1=5$ ms, $\tau_2=3,75$ ms, $\tau_3=2,5$ ms and the input time-delays are $\tau_4=\tau_5=\tau_6=2,5$ ms for time interval $1,5\ \text{s}\leq t\leq 3,5$ s. The resulting data set for this context is shown in Fig. 1. The goal is to design the interval type-2 fuzzy Kalman filter for filtering and tracking the reference trajectory $\mathbf{r}(t)$ considering failing data.

The first 200 samples were used in training step for initial parameterization of interval type-2 fuzzy Kalman filter. The unobservable components associated to state variables x_1, x_2 and x_3 of Chen's chaotic attractor were extracted by singular spectral analysis approach, according Sect. 3.1, for preprocessing of data set. The noisy state variables x_1, x_2 and x_3 were decomposed into 2 spectral components which are shown in Figs. 2, 3 and 4. The α^2 component, extracted from each state variable, assuming correlated to nominal dynamic of state variables x_1, x_2 and x_3, was used for parameterizing the interval type-2 fuzzy Kalman filter.

The weighting matrix $\boldsymbol{\mathcal{X}}_k$ for implementing the recursive updating mechanism of interval type-2 fuzzy Kalman filter is defined as identity matrix as applied for filtering and tracking the reference trajectory $\mathbf{r}(t)$. The partitions of computational data from noisy variable $\mathbf{Z}=\left[x_1\ \ x_2\ \ x_3\right]^T$ were defined by interval type-2 fuzzy Gustafson-Kessel clustering algorithm, so the antecedent proposition, the rules number, and

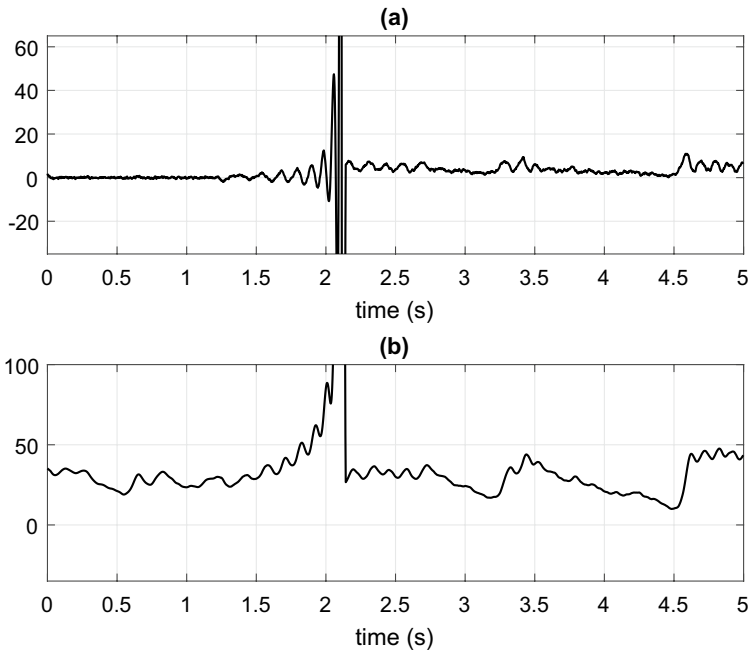

Fig. 4 The spectral components $\alpha^j|^{j=1,\ldots,2}$, which were extracted for state variable x_3 from Chen's chaotic attractor: **a** α^1; **b** α^2

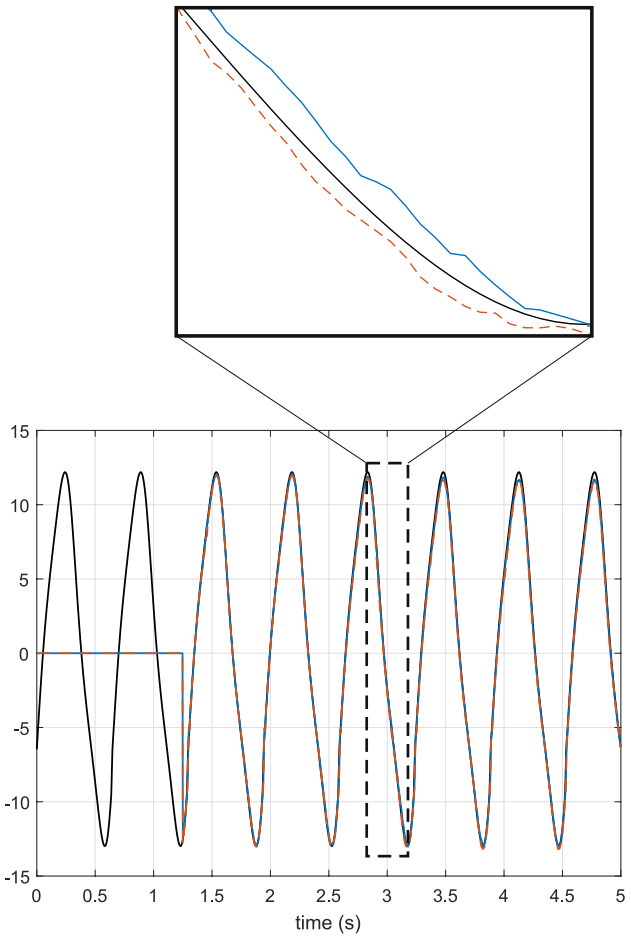

Fig. 5 The confidence region obtained for filtering and tracking the reference trajectory $r_1(t)$ by state variable x_1 of Chen's chaotic attractor

consequent proposition, of the interval type-2 fuzzy Kalman filter, could be estimated successfully. For implementing the interval type-2 fuzzy clustering algorithm, the following parameters were adopted: number of clusters $c = 2$, interval weighting exponent $\widetilde{m} = [1,5 \;\; 2]$ and termination tolerance $\mathcal{E} = 10^{-5}$. The parametric estimation of consequent proposition of interval type-2 fuzzy Kalman filter inference system, in Eq. 15, took into account the partitions on noisy variable $\mathbf{Z} = \left[x_1 \;\; x_2 \;\; x_3\right]^T$ as weighting criterion, and the parameters values: $q = 1$, $\gamma = 10$ e $\beta = 10$. The confidence regions, as shown in Figs. 5, 6 and 7, created by interval type-2 fuzzy Kalman filter taking into account uncertainties, estimated by interval type-2 membership functions inherited to noisy data from Chen's chaotic attractor, illustrates its efficiency for tracking the reference trajectory $\mathbf{r}(t)$.

The estimation of the temporal behavior of main diagonal elements from interval type-2 fuzzy Kalman gain matrix $\widetilde{\mathbf{K}}^i$ during recursive updating of interval type-2 fuzzy Kalman filter for filtering and tracking the reference trajectory $\mathbf{r}(t)$, is shown in Figs. 8, 9.

The upper and lower instantaneous activation degrees related to interval type-2 fuzzy Kalman filter inference system, during its training and recursive steps, for filtering and tracking the reference trajectory $\mathbf{r}(t)$ through state variables of Chen's chaotic attractor, are shown in Fig. 10.

The efficiency of interval type-2 fuzzy Kalman filter algorithm as compared to approach (Wu et al. 2015) and others clustering algorithms (Fuzzy C-Means and Possibilistic C-Means), for filtering and tracking the reference trajectory $\mathbf{r}(t)$ through state variables of Chen's chaotic attractor,

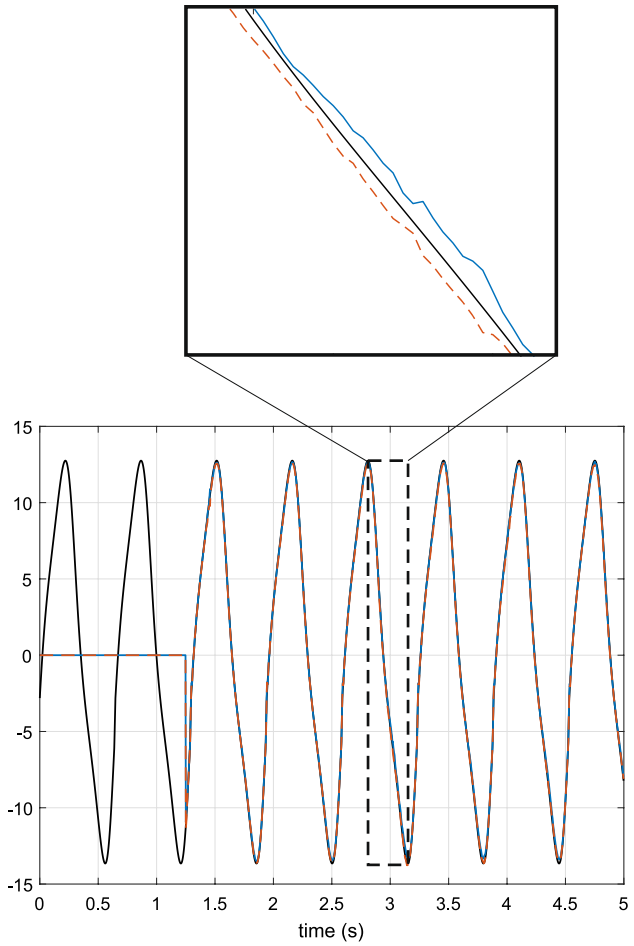

Fig. 6 The confidence region obtained for filtering and tracking the reference trajectory $r_2(t)$ by state variable x_2 of Chen's chaotic attractor

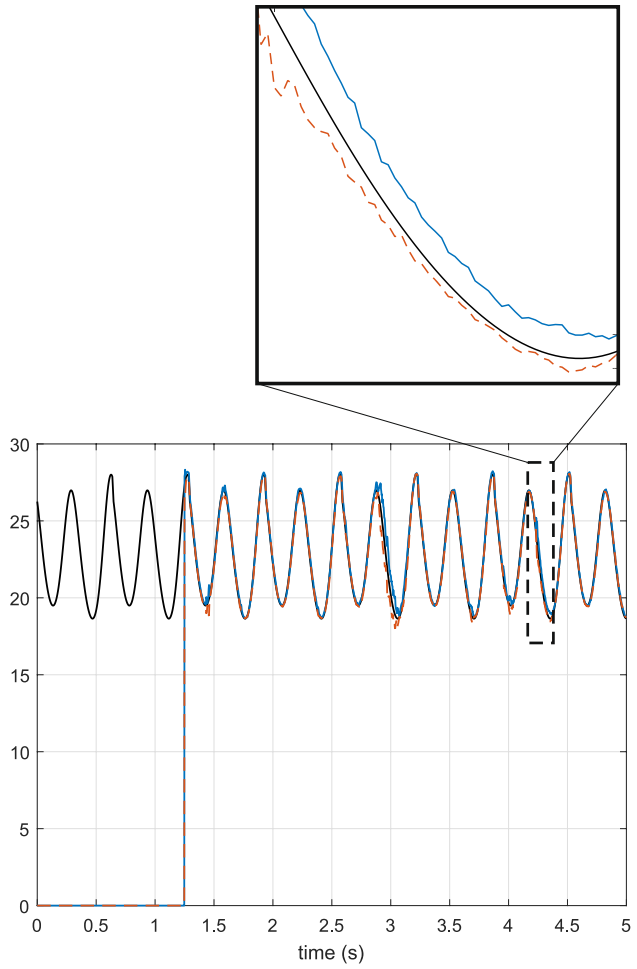

Fig. 7 The confidence region obtained for filtering and tracking the reference trajectory $r_3(t)$ by state variable x_3 of Chen's chaotic attractor

based on Mean Absolute Error (MAE) validation criterion, is shown in Table 1.

4.2 Experimental results

In this section, experimental results for forecasting analysis of dynamic spread behavior taking into account the experimental data of daily deaths reports caused by Covid-19 in Brazil, are presented.

4.2.1 Interval type-2 fuzzy Kalman filtering and forecasting analysis of the dynamic spread of COVID-19 in Brazil

The experimental data corresponding to daily deaths reports within the period ranging from 29 of February 2020 to 18 of May 2020, in Brazil, is shown in Fig. 11. Once that the problem of interest, in this paper, is based on the time series related to daily deaths reports in Brazil, the variable $\mathbf{u}_k$, in Eq. 15 of proposed methodology, is considered as white noise signal with low amplitude.

The pre-processing of experimental data by singular spectral analysis, was able for extracting the unobservable components associated to daily deaths reports. The Variance Accounted For (VAF) was considered as criterion for evaluating the appropriate number of these components, within a range from 2 to 15 ones, for best representation of the experimental data, as shown in Fig. 12.

As it can be seen, considering the cost-benefit balance for computational practical application of the proposed methodology, the appropriated number of unobservable components was $\xi = 10$, with VAF value of 99,98% in efficiency to represent as accurately as possible the experimental data and, at same time, reducing the computational load of interval type-2 fuzzy Kalman filter algorithm. The illustration of spectral unobservable components α^1 and α^{10}, which were extracted from daily deaths reports in Brazil, are shown in Fig. 13.

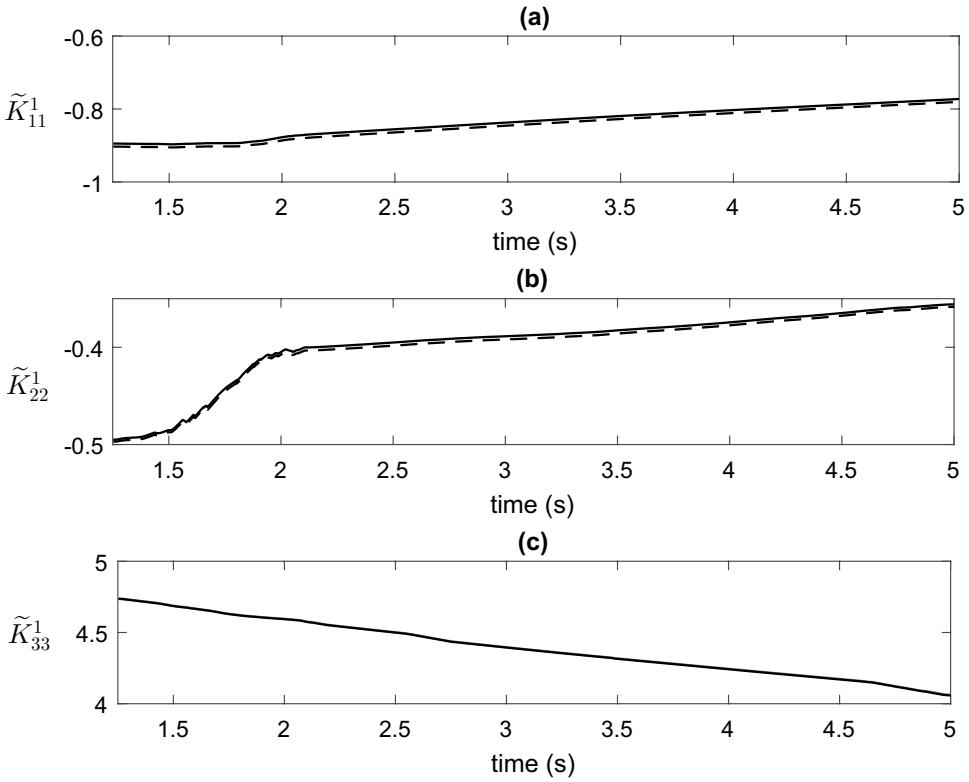

Fig. 8 Interval type-2 fuzzy Kalman gain matrix of rule 1 for filtering and tracking the reference trajectory $\mathbf{r}(t)$: **a** $\widetilde{K}_{11}^{1}$, **b** $\widetilde{K}_{22}^{1}$, **c** $\widetilde{K}_{33}^{1}$

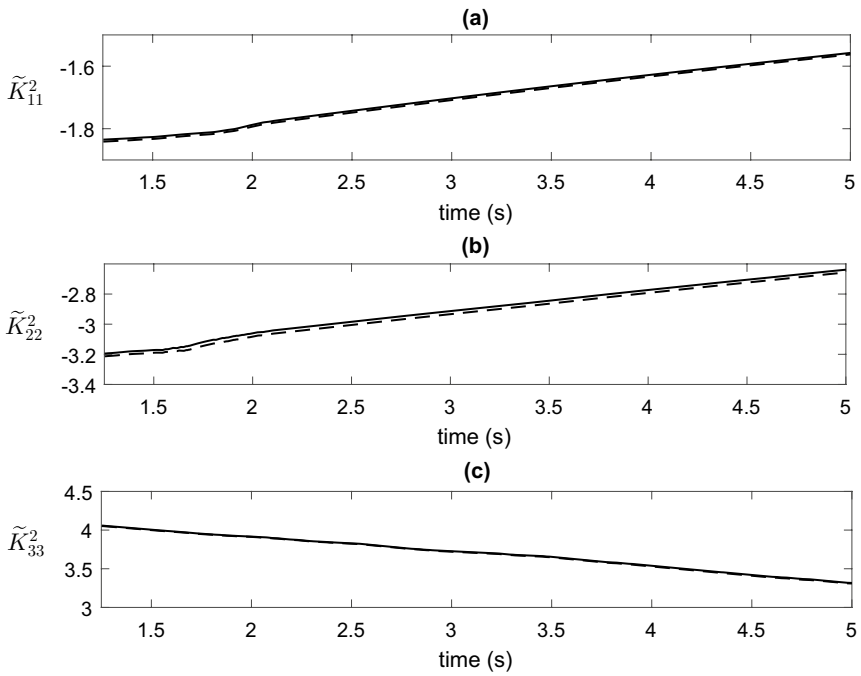

Fig. 9 Interval type-2 fuzzy Kalman gain matrix of rule 2 for filtering and tracking the reference trajectory $\mathbf{r}(t)$: **a** $\widetilde{K}_{11}^{2}$, **b** $\widetilde{K}_{22}^{2}$, **c** $\widetilde{K}_{33}^{2}$

The partitions of experimental data related to daily deaths reports were defined by interval type-2 fuzzy Gustafson-Kessel clustering algorithm, as shown in Fig. 14, so the antecedent proposition, the rules number, and consequent proposition, of the type-2 fuzzy Kalman filter, could be estimated successfully. For implementing the proposed type-2 fuzzy clustering algorithm, the following parameters were adopted: number of clusters $c = 3$, interval weighting exponent $\widetilde{m} = [1,5 \;\; 2,3]$ and termination tolerance $\mathcal{E} = 10^{-5}$.

The implementation of interval type-2 fuzzy OKID algorithm, for parametric estimation of consequent proposition in the type-2 fuzzy Kalman filter inference system, in Eq. 15,

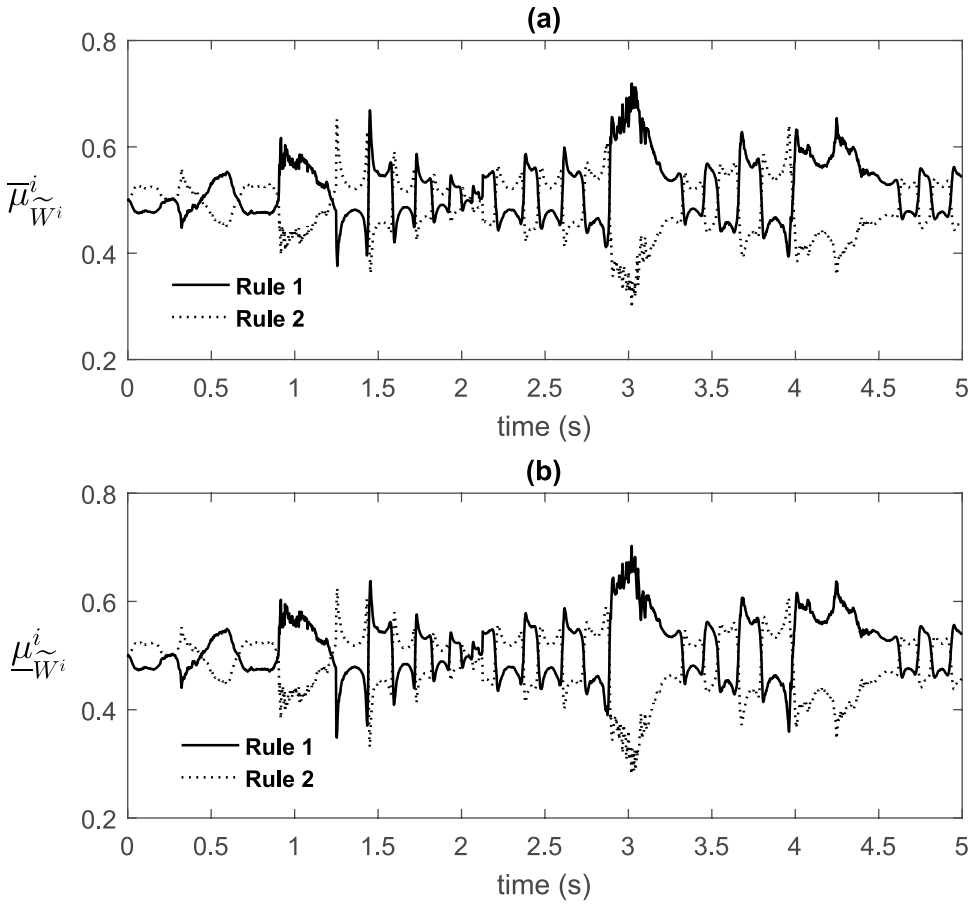

Fig. 10 Instantaneous normalized fuzzy activation degrees: **a** upper activation degrees; **b** lower activation degrees

Table 1 Performance of interval type-2 fuzzy Kalman filter algorithm as compared to (Wu et al. 2015) and others clustering algorithms (Fuzzy C-Means and Possibilistic C-Means), for filtering and tracking the reference trajectory $\mathbf{r}(t)$ through state variables of Chen's chaotic attractor

	$\text{MAE}_{r_1(t)}$	$\text{MAE}_{r_2(t)}$	$\text{MAE}_{r_3(t)}$
Approach in Wu et al. (2015)	403.92	555.41	415.14
Fuzzy C-Means clustering algorithm	0.3793	0.5209	0.8221
Possibilistic C-Means clustering algorithm	0.5830	0.4892	0.4202
Lower limit of interval type-2 fuzzy Kalman filter	0.3435	0.0308	0.1800
Upper limit of interval type-2 fuzzy Kalman filter	0.3166	0.0205	0.5843

took into account the partitions on daily deaths reports, in Fig 14, as weighting criterion, and the parameters values: $q = 1$, $\gamma = 15$ e $\beta = 15$. According to experimental data of daily deaths reports in Brazil shown in Fig. 11, the pre-processed unobservable components shown in Fig. 13, the interval type-2 fuzzy normalized membership values shown in Fig. 14, the initial parametric estimation of the type-2 fuzzy Kalman filter was computed by training step. The confidence region, as shown in Fig. 15, created by initial estimation of interval type-2 fuzzy Kalman filter taking into account uncertainties estimated by interval type-2 membership functions shown in Fig. 14, inherited to experimental data ranging from 29 of February 2020 to 18 of May 2020, illustrates its efficiency for tracking the experimental data of daily deaths reports in Brazil.

From this confidence region, shown in Fig. 15, an interval normal distribution projections were estimated, delimiting upper and lower limits for forecasting the future daily deaths reports in Brazil. The efficiency of interval type-2 fuzzy Kalman filter based on its initial estimation by training step from experimental data of daily deaths reports ranging from 29 of February 2020 to 18 of May 2020, for forecasting the future (validation) experimental data of daily deaths reports within the period ranging from 19 of May 2020 to 27 of May

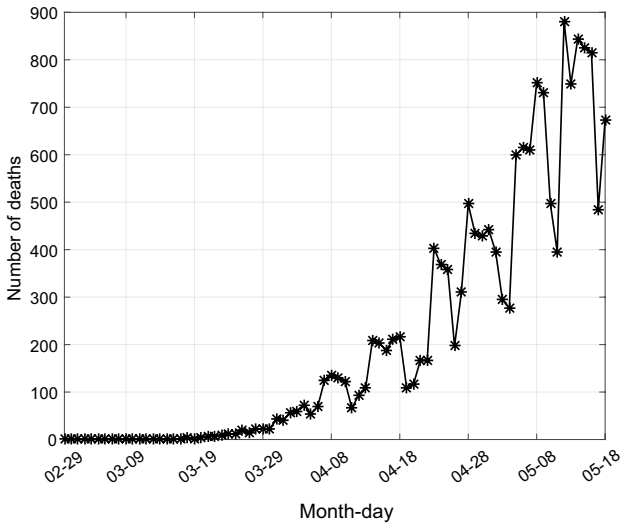

Fig. 11 The experimental data of daily deaths reports within period from 29 of February 2020 to 18 of May 2020, in Brazil

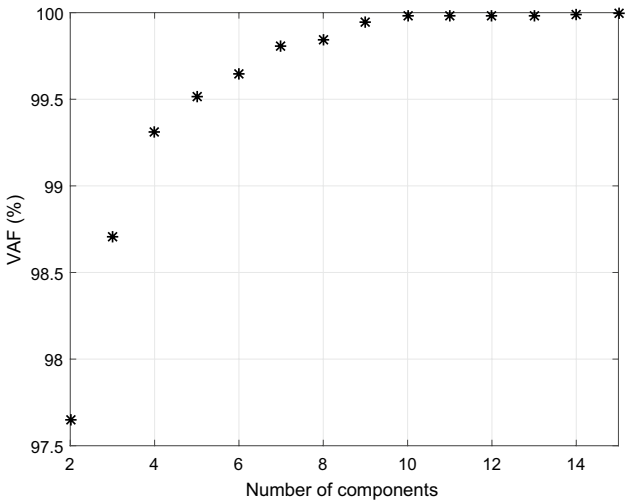

Fig. 12 The efficiency of unobservable components for representing the experimental data of the daily deaths reports, in Brazil

2020, is shown in Fig. 16a. The new recursive updating of interval type-2 fuzzy Kalman filter on 27 of May 2020, for proposals of new tracking and forecasting future daily deaths reports within the period ranging from 28 of May 2020 to 24 of June 2020, is shown in Fig. 16b. The new recursive updating of the interval type-2 fuzzy Kalman filter was on 24 of June 2020, for proposals of new tracking and forecasting future daily deaths reports within the period ranging from 25 of June 2020 to 30 of June 2020, is shown in Fig. 16c. The new recursive updating of the interval type-2 fuzzy Kalman filter was on 30 of June 2020, for proposals of new tracking and forecasting future daily deaths reports within the period ranging from 01 of July 2020 to 15 of July 2020, is shown in Fig. 16d. The new recursive updating of the interval type-2 fuzzy Kalman filter was on 15 of July 2020, for proposals of new tracking and forecasting future daily deaths reports within the period ranging from 16 of July 2020 to 23 of July 2020, is shown in Fig. 16e. The new recursive updating of the interval type-2 fuzzy Kalman filter was on 23 of July 2020, for proposals of new tracking and forecasting future daily deaths reports within the period ranging from 24 of July 2020 to ahead, is shown in Fig. 16f. It can be seen an efficiency in the adaptability of interval normal distribution projections created in real time by interval type-2 fuzzy Kalman filter, which illustrates its applicability for tracking and forecasting the COVID-19 dynamic spread experimental data related to daily deaths reports in Brazil.

The estimation of interval type-2 fuzzy Kalman gain matrices $\widetilde{\mathbf{K}}^i|^{i=1,\ldots,3}$, during recursive updating of interval type-2 fuzzy Kalman filter, within period ranging from 19 of May 2020 to 23 of July 2020, in Brazil, is shown in Fig. 17.

The upper and lower instantaneous activation degrees related to interval type-2 fuzzy Kalman filter inference system, during its training and recursive steps within period ranging from 29 of February 2020 to 23 of July 2020, in Brazil, are shown in Fig. 18.

The efficiency of interval type-2 fuzzy Kalman filter, during its recursive updating for tracking and forecasting the COVID-19 dynamic spread experimental data related to daily deaths reports within period ranging from 18 of May 2020 to 27 of July 2020, in Brazil, was validated through Variance Accounted For (VAF) criterion, as shown in Fig. 19.

4.3 Comparative analysis and discussions

In this section, a more detailed discussion on the results shown in Sect. 4.2.1, according to comparative analysis of proposed methodology with the approaches in Feroze (2020), Hazarika and Gupta (2020), considering the metrics RMSE (Root Mean Square Error), MAE (Mean Absolute Error), RMSPE (Root Mean Square Percentage Error) and coefficient of determination (R^2), is presented.

The approach in Feroze (2020) is based on Bayesian structural time series (BSTS) models for forecasting the COVID-19 dynamic propagation in Brazil, within the horizon of 30 days. The efficiency of interval type-2 fuzzy Kalman filter, compared to approach proposed in Feroze (2020), is shown in Table 2. As it can be seen, although the Bayesian model in approach (Feroze 2020) be adaptive, it presents a inferior performance compared to interval type-2 fuzzy Kalman filter, once that it is based on Bayesian

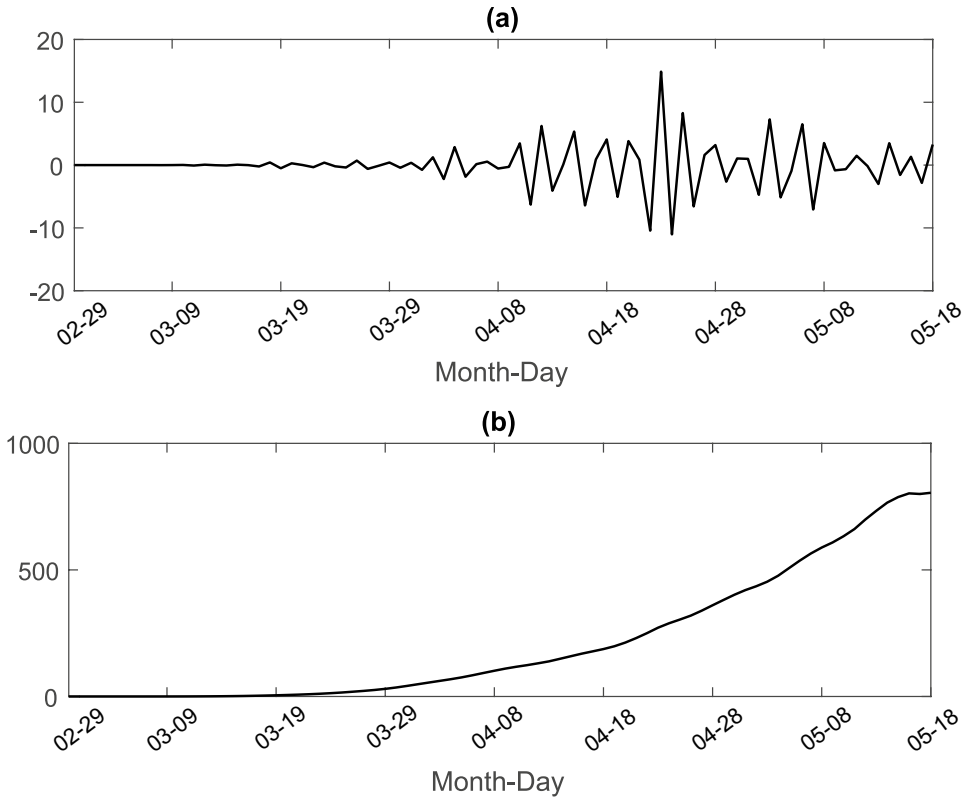

Fig. 13 The spectral unobservable components extracted from daily deaths reports in Brazil : **a** α^1 and **b** α^{10}

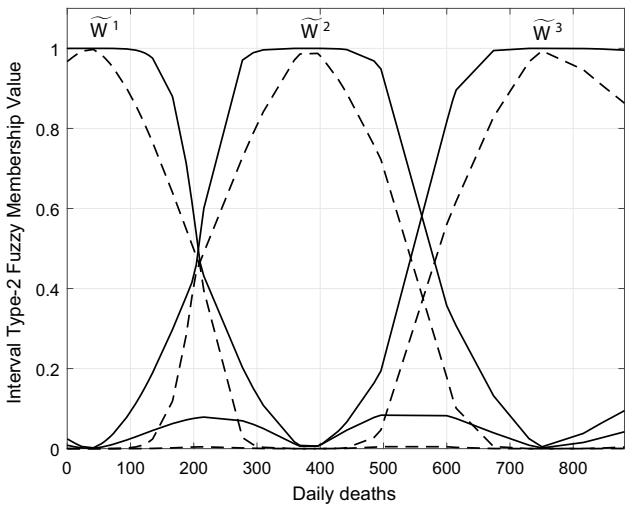

Fig. 14 Interval type-2 fuzzy membership functions estimated from clustering of daily deaths reports, in Brazil

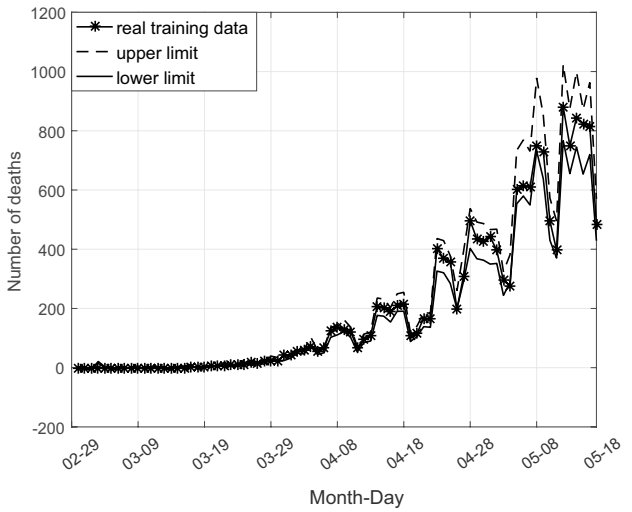

Fig. 15 The confidence region resulted from tracking the experimental data of daily deaths reports, from 29 of February 2020 to 18 of May 2020, in Brazil

inference mechanism influenced by previously computed probability distributions, which contributes for increasing the forecasting errors (Berger 1993).

The approach in Hazarika and Gupta (2020) is based on Wavelet-Coupled Random Vector Functional Link (WCRVFL) network for forecasting the COVID-19 dynamic

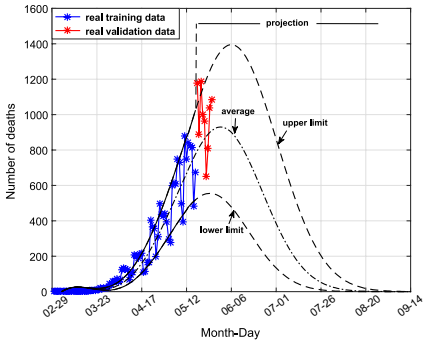

(a) Forecasting within the period ranging from 19 of May 2020 to 27 of May 2020, in Brazil.

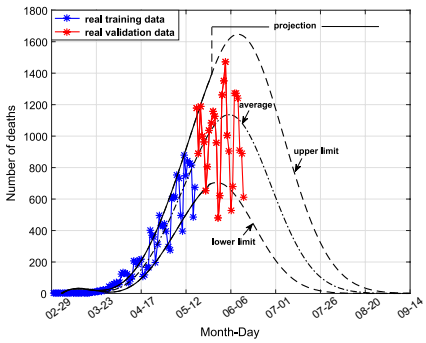

(b) Forecasting within the period ranging from 28 of May 2020 to 24 of June 2020, in Brazil

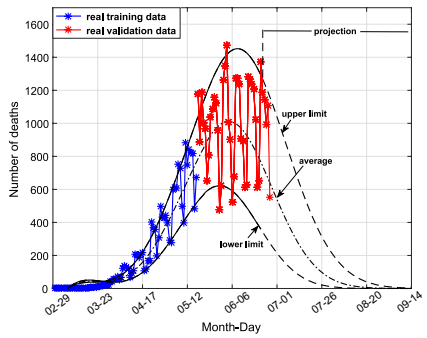

(c) Forecasting within the period ranging from 25 of June 2020 to 30 of June 2020, in Brazil.

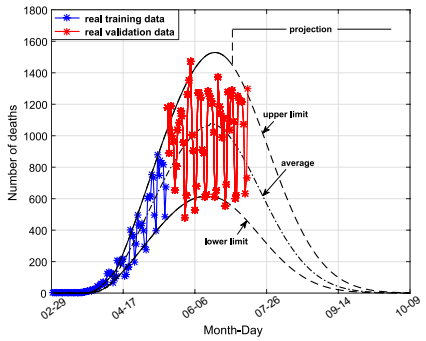

(d) Forecasting within the period ranging from 01 of July to 15 of July 2020, in Brazil.

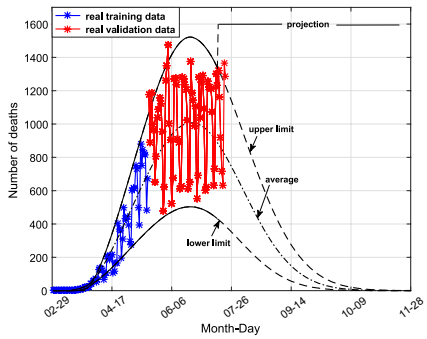

(e) Forecasting within the period ranging from 16 of July 2020 to 23 of July 2020, in Brazil.

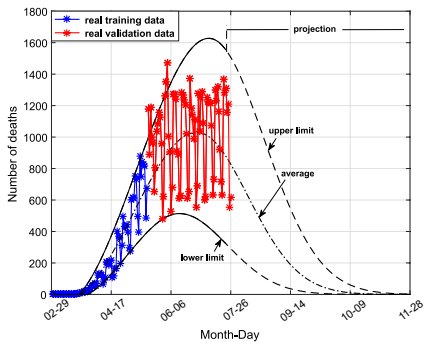

(f) Forecasting within the period ranging from 24 of July 2020 to ahead, in Brazil.

Fig. 16 Performance of the interval type-2 fuzzy Kalman filter for tracking and forecasting the COVID-19 related to daily deaths reports, in Brazil

propagation in Brazil, within the horizon of 60 days, using a normalization procedure of dataset from the following formulation:

$$\breve{z}_k = \frac{z_k - min(\mathbf{Z})}{max(\mathbf{Z}) - min(\mathbf{Z})}, \quad k = 1, 2, \ldots, k_{currrent} \tag{70}$$

where $\mathbf{Z} = \left[z_1, z_2, \ldots, z_{k_{current}}\right]^T$ is the experimental dataset, $\breve{z}_k$ is the normalized value of z_k, $min(\mathbf{Z})$ is the minimum value of $\mathbf{Z}$, $max(\mathbf{Z})$ is the maximum value of $\mathbf{Z}$, and $k_{currrent}$ is the time for acquisition of the current experimental data $z_{k_{current}}$. The normalization procedure is performed throughout the fluctuations of experimental data defined on a temporal window ($k = 1, 2, \ldots, k_{currrent}$), so that $min(\mathbf{Z})$ and $max(\mathbf{Z})$ values are guaranteed for solution of Eq. (70) (?) . The efficiency of interval type-2 fuzzy Kalman filter, compared to approach in (Hazarika and Gupta 2020), is shown in Table 3. As it can be seen, once that the approach in (Hazarika and Gupta 2020) uses different types of wavelets to process non-stationarity

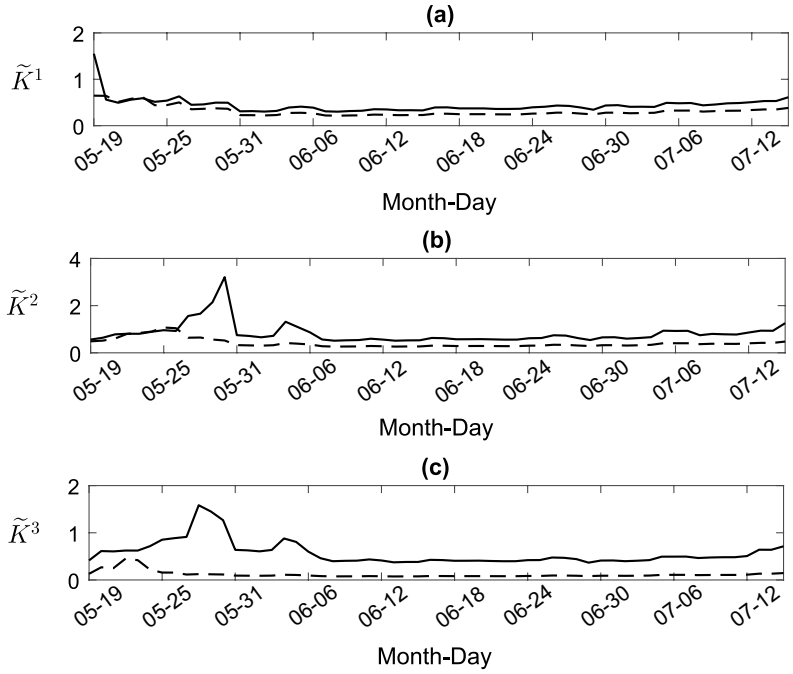

Fig. 17 Interval type-2 fuzzy Kalman gains, for tracking and forecasting the COVID-19 dynamic spread behavior: **a** Rule 1, **b** Rule 2, **c** Rule 3

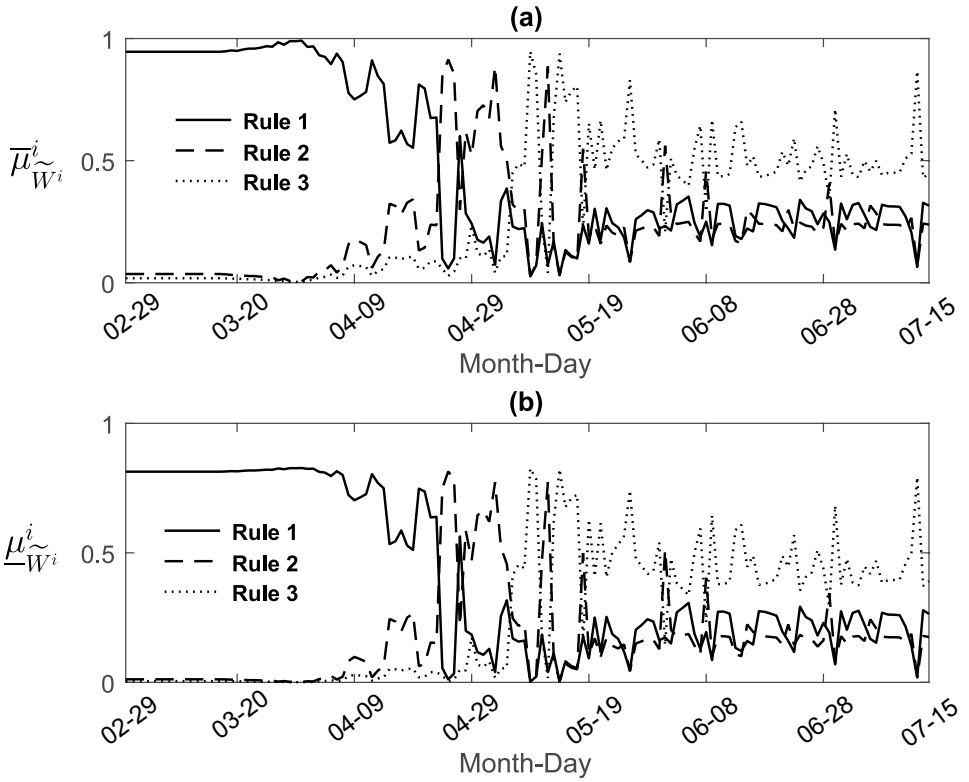

Fig. 18 Instantaneous normalized fuzzy activation degrees: **a** upper activation degrees, **b** lower activation degrees

of experimental dataset, it presents competitive results compared to interval type-2 fuzzy Kalman filter, but the performance is slightly inferior due to its computing limitation from determination of the optimal number of nodes in the hidden layer of the WCRVFL network, tuning the scaling of the uniform randomization range for wavelet estimator and accurate data availability.

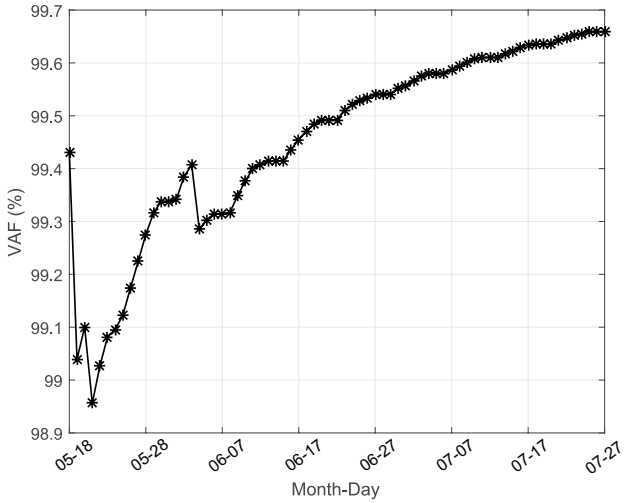

Fig. 19 Real time efficiency of interval type-2 fuzzy Kalman filter, within period ranging from 18 of May 2020 to 27 of July 2020, in Brazil

Table 2 Comparative analysis between the interval type-2 fuzzy Kalman filter and approach in Feroze (2020) for forecasting the COVID-19 dynamic propagation in Brazil

Methodology	RMSE	MAE	RMSPE	R^2
Approach in (Feroze 2020)	3669,000	2533	0.0873	0.657
Interval type-2 *fuzzy* Kalman filter	531,472	97	0.0249	0.989

Table 3 Comparative analysis between the interval type-2 fuzzy Kalman filter and approach in Hazarika and Gupta (2020) for forecasting the COVID-19 dynamic propagation in Brazil

Methodology	RMSE	MAE	RMSPE	R^2
Approach in (Hazarika and Gupta 2020)	0.00619	0.00488	0.23590	0.99945
Interval type-2 *fuzzy* Kalman filter	0.00338	0.00070	0.00339	0.99967

5 Conclusion

In this paper, an approach for experimental data based design of Interval Type-2 Fuzzy Kalman Filters, was proposed. Computational results shown efficiency of designed interval type-2 fuzzy Kalman filter, as compared to another approaches widely cited in the literature, for filtering and tracking the reference trajectory through state variables of Chen's chaotic attractor in noisy environment and time delays. Experimental results shown the applicability of interval type-2 fuzzy Kalman filter, according to proposed methodology, due to its recursive updating mechanism, for adaptive and real time forecasting the COVID-19 spreading dynamic related to daily deaths reports in Brazil. From the recursive updating on 23 of July 2020, it could be inferred by forecasting interval projections the month of September as more adequate for reassessment the requirements on flexibility of social activities in Brazil (containing the 27 states and federal district). For further works, the formulation and applicability of proposed methodology in the context of evolving interval type-2 fuzzy systems, is of particular interest.

Acknowledgements This work was developed in the Laboratory of Computational Intelligence Applied to Technology at Federal Institute of Education, Science and Technology of Maranhão. The authors are grateful to Coordination for the Improvement of Higher Education Personnel (CAPES) for financial support and to the Master and Doctorate Program in Electrical Engineering at Federal University of Maranhão (PPGEE-UFMA) for their support in the development of this research.

References

Antsaklis PJ, Astolfi A (2020) Realizations in linear systems theory. In: Encyclopedia of systems and control. Springer London, pp 1–5, https://doi.org/10.1007/978-1-4471-5102-9_193-2

Asl RM, Palm R, Wu H, Handroos H (2020) Fuzzy-based parameter optimization of adaptive unscented Kalman filter: methodology and experimental validation. IEEE Access 8:54887–54904. https://doi.org/10.1109/access.2020.2979987

Babuska R (1998) Fuzzy modeling control. Kluwer Academic Publishers, New York

Bendat (1998) Nonlinear system techniques. Wiley, Hoboken

Berger JO (1993) Statistical decision theory and bayesian analysis. Springer, New York

Bonyadi MR, Michalewicz Z (2016) Analysis of stability, local convergence, and transformation sensitivity of a variant of the particle swarm optimization algorithm. IEEE Trans Evol Comput 20(3):370–385. https://doi.org/10.1109/tevc.2015.2460753

Bouhentala M, Ghanai M, Chafaa K (2019) Interval-valued membership function estimation for fuzzy modeling. Fuzzy Sets Syst 361:101–113. https://doi.org/10.1016/j.fss.2018.06.008

Boutayeb M, Rafaralahy H, Darouach M (1997) Convergence analysis of the extended Kalman filter used as an observer for nonlinear deterministic discrete-time systems. IEEE Trans Autom Control 42(4):581–586. https://doi.org/10.1109/9.566674

Callier FM, Desoer CA (1991) Realization theory. In: Springer texts in electrical engineering. Springer New York, pp 295–314, https://doi.org/10.1007/978-1-4612-0957-7_13

Chan SC, Lin JQ, Sun X, Tan HJ, Xu WC (2020) A new variable forgetting factor-based bias-compensation algorithm for recursive identification of time-varying multi-input single-output systems with measurement noise. IEEE Trans Instrum Meas 69(7):4555–4568. https://doi.org/10.1109/tim.2019.2947121

Chen CT (1999) Linear system theory and design. Oxford University Press, Oxford

Chen L, Mercorelli P, Liu S (2005) A Kalman estimator for detecting repetitive disturbances. Proc Am Control Conf IEEE 3:1631–1636. https://doi.org/10.1109/acc.2005.1470201

Elsner JB (2002) Analysis of time series structure: SSA and related techniques. J Am Stat Assoc 97(460):1207–1208. https://doi.org/10.1198/jasa.2002.s239

Evangelista APF, Serra GLO (2019) Multivariable state-space recursive identification algorithm based on evolving type-2 neural-fuzzy inference system. J Control Autom Electric Syst 30(6):921–942. https://doi.org/10.1007/s40313-019-00528-0

Evangelista APF, Serra GLO (2020) State space black-box modelling via Markov parameters based on evolving type-2 neural-fuzzy inference system for nonlinear multivariable dynamic systems. Fuzzy Sets Syst 394:1–39. https://doi.org/10.1016/j.fss.2019.08.013

Eyoh I, John R, Maere GD, Kayacan E (2018) Hybrid learning for interval type-2 intuitionistic fuzzy logic systems as applied to identification and prediction problems. IEEE Trans Fuzzy Syst 26(5):2672–2685. https://doi.org/10.1109/tfuzz.2018.2803751

Feroze N (2020) Forecasting the patterns of COVID-19 and causal impacts of lockdown in top five affected countries using Bayesian structural time series models. Chaos Solitons Fractals 140:110196. https://doi.org/10.1016/j.chaos.2020.110196

Gil P, Oliveira T, Palma L (2019) Adaptive neuro–fuzzy control for discrete-time nonaffine nonlinear systems. IEEE Trans Fuzzy Syst 27(8):1602–1615. https://doi.org/10.1109/tfuzz.2018.2883540

Gilbert JA, Meyers LA, Galvani AP, Townsend JP (2014) Probabilistic uncertainty analysis of epidemiological modeling to guide public health intervention policy. Epidemics 6:37–45. https://doi.org/10.1016/j.epidem.2013.11.002

Gomez-Garcia R, Yang L, Munoz-Ferreras JM, Feng W (2020) Lossy signal-interference filters and applications. IEEE Trans Microw Theory Tech 68(2):516–529. https://doi.org/10.1109/tmtt.2019.2953585

Haessig D, Friedland B (1998) Separate-bias estimation with reduced-order Kalman filters. IEEE Trans Autom Control 43(7):983–987. https://doi.org/10.1109/9.701106

Hangos KM, Bokor J, Szederkényi G (2004) Analysis and control of nonlinear process systems. Springer-Verlag, Berlin, pp 73–96. https://doi.org/10.1007/1-85233-861-x_5

Hazarika BB, Gupta D (2020) Modelling and forecasting of COVID-19 spread using wavelet-coupled random vector functional link networks. Appl Soft Comput 96:106626. https://doi.org/10.1016/j.asoc.2020.106626

Heintzman N, Kleinberg S (2016) Using uncertain data from body-worn sensors to gain insight into type 1 diabetes. J Biomed Inf 63:259–268. https://doi.org/10.1016/j.jbi.2016.08.022

Hendricks E, Jannerup O, Sorensen PH (2008) Linear systems control: deterministic and stochastic methods. Springer, Berlin. https://doi.org/10.1007/978-3-540-78486-9

Hsieh CS (2000) Robust two-stage Kalman filters for systems with unknown inputs. IEEE Trans Autom Control 45(12):2374–2378. https://doi.org/10.1109/9.895577

Huang Y, Zhang Y, Wu Z, Li N, Chambers J (2018) A novel adaptive Kalman filter with inaccurate process and measurement noise covariance matrices. IEEE Trans Autom Control 63(2):594–601. https://doi.org/10.1109/tac.2017.2730480

Hurtik P, Molek V, Hula J (2020) Data preprocessing technique for neural networks based on image represented by a fuzzy function. IEEE Trans Fuzzy Syst 28(7):1195–1204. https://doi.org/10.1109/tfuzz.2019.2911494

Hwang CL, Wu HM, Lai JY (2019) On-line obstacle detection, avoidance, and mapping of an outdoor quadrotor using EKF-based fuzzy tracking incremental control. IEEE Access 7:160203–160216. https://doi.org/10.1109/access.2019.2950324

Juang JN (1994) Applied system identification. Prentice Hall, Hoboken

Kalman RE (1960) A new approach to linear filtering and prediction problems. J Basic Eng 82(1):35–45. https://doi.org/10.1115/1.3662552

Khairalla M, Ning X, AL-Jallad JN (2018) Modelling and optimisation of effective hybridisation model for time-series data forecasting. J Eng 2:117–122. https://doi.org/10.1049/joe.2017.0337

Khanesar MA, Kayacan E, Teshnehlab M, Kaynak O (2012) Extended Kalman filter based learning algorithm for type-2 fuzzy logic systems and its experimental evaluation. IEEE Trans Ind Electron 59(11):4443–4455. https://doi.org/10.1109/tie.2011.2151822

Khayyam H, Jamali A, Bab-Hadiashar A, Esch T, Ramakrishna S, Jalili M, Naebe M (2020) A novel hybrid machine learning algorithm for limited and big data modeling with application in industry 4.0. IEEE Access 8:111381–111393. https://doi.org/10.1109/access.2020.2999898

Lan LTH, Tuan TM, Ngan TT, Son LH, Giang NL, Ngoc VTN, Hai PV (2020) A new complex fuzzy inference system with fuzzy knowledge graph and extensions in decision making. IEEE Access 8:164899–164921. https://doi.org/10.1109/access.2020.3021097

Liang Q, Mendel J (2000) Interval type-2 fuzzy logic systems: theory and design. IEEE Trans Fuzzy Syst 8(5):535–550. https://doi.org/10.1109/91.873577

Lin CT, Pal NR, Wu SL, Liu YT, Lin YY (2015) An interval type-2 neural fuzzy system for online system identification and feature elimination. IEEE Trans Neural Netw Learn Syst 26(7):1442–1455. https://doi.org/10.1109/tnnls.2014.2346537

Liu W, Liu Y, Bucknall R (2019) A robust localization method for unmanned surface vehicle (USV) navigation using fuzzy adaptive Kalman filtering. IEEE Access 7:46071–46083. https://doi.org/10.1109/access.2019.2909151

Ma Z, Ma H (2020) Adaptive fuzzy backstepping dynamic surface control of strict-feedback fractional-order uncertain nonlinear systems. IEEE Trans Fuzzy Syst 28(1):122–133. https://doi.org/10.1109/tfuzz.2019.2900602

Mack W, Habets EAP (2020) Deep filtering: signal extraction and reconstruction using complex time-frequency filters. IEEE Signal Process Lett 27:61–65. https://doi.org/10.1109/lsp.2019.2955818

Martynyuk AA, Yu A, Martynyuk-Chernienko (2019) Uncertain dynamical systems: stability and motion control. CRC Press, Boca Roton

Mendel JM (2019) Comparing the performance potentials of interval and general type-2 rule-based fuzzy systems in terms of sculpting the state space. IEEE Trans Fuzzy Syst 27(1):58–71. https://doi.org/10.1109/tfuzz.2018.2856184

Moss F, McClintock PVE (1989) Noise in nonlinear dynamical systems. Cambridge University Press, Cambridge. https://doi.org/10.1017/cbo9780511897818

Pires DS, Serra GL (2020) Methodology for modeling fuzzy Kalman filters of minimum realization from evolving clustering of experimental data. ISA Trans. https://doi.org/10.1016/j.isatra.2020.05.034

Pires DS, Serra GLO (2019) Methodology for evolving fuzzy Kalman filter identification. Int J Control Autom Syst 17(3):793–800. https://doi.org/10.1007/s12555-017-0503-6

Schimmack M, Haus B, Mercorelli P (2018) An extended Kalman filter as an observer in a control structure for health monitoring of a metal–polymer hybrid soft actuator. IEEE/ASME Trans Mechatron 23(3):1477–1487. https://doi.org/10.1109/tmech.2018.2792321

Schoukens J, Ljung L (2019) Nonlinear system identification: a user-oriented road map. IEEE Control Syst Mag. https://doi.org/10.1109/MCS.2019.2938121

Serra GLO (2018) Kalman filters—theory for advanced applications. InTech, London. https://doi.org/10.5772/intechopen.68249

Taghavifar H (2020) EKF estimation based PID type-2 fuzzy control of electric cars. Measurement. https://doi.org/10.1016/j.measurement.2020.108557

Tang G, Wu Y, Li C, Wong PK, Xiao Z, An X (2020) A novel wind speed interval prediction based on error prediction method. IEEE Trans Ind Inf 16(11):6806–6815. https://doi.org/10.1109/tii.2020.2973413

Tomás-Rodríguez M, Banks SP (2010) Linear, time-varying approximations to nonlinear dynamical systems. Springer, London. https://doi.org/10.1007/978-1-84996-101-1

Wang LY, Zhao WX (2013) System identification: new paradigms, challenges, and opportunities. Acta Autom Sin 39(7):933–942. https://doi.org/10.1016/s1874-1029(13)60062-2

Wang X, Xu Z, Gou X, Trajkovic L (2020) Tracking a maneuvering target by multiple sensors using extended Kalman filter with nested probabilistic-numerical linguistic information. IEEE Trans Fuzzy Syst 28(2):346–360. https://doi.org/10.1109/tfuzz.2019.2906577

Wu CY, Tsai JH, Guo SM, Shieh LS, Canelon J, Ebrahimzadeh F, Wang L (2015) A novel on-line observer/Kalman filter identification method and its application to input-constrained active fault-tolerant tracker design for unknown stochastic systems. J Franklin Inst 352(3):1119–1151. https://doi.org/10.1016/j.jfranklin.2014.12.004

Zhang L, Lam HK, Sun Y, Liang H (2020) Fault detection for fuzzy semi-Markov jump systems based on interval type-2 fuzzy approach. IEEE Trans Fuzzy Syst 28(10):2375–2388. https://doi.org/10.1109/tfuzz.2019.2936333

Zhu X, Wang T, Bao Y, Hu F, Li S (2019) Signal detection in generalized gaussian distribution noise with Nakagami fading channel. IEEE Access 7:23120–23126. https://doi.org/10.1109/access.2019.2895627